DOI:
10.1242/dev.153387

Document Version
Peer reviewed version

Development Advance Online Articles. First posted online on 14 August 2017 as 10.1242/dev.153387
Access the most recent version at http://dev.biologists.org/lookup/doi/10.1242/dev.153387

Hypothalamic sonic hedgehog is required for cell specification and proliferation of LHX3/LHX4 pituitary embryonic precursors

G. Carreno[1], J. Apps[1], E.J. Lodge[2], L. Panousopoulos[1], S. Haston[1], J.M. Gonzalez-Meljem[1], H. Hahn [3], C.L. Andoniadou[2,4], J.P. Martinez-Barbera[1,*]

1. Developmental Biology and Cancer Programme, Birth Defects Research Centre, Great Ormond Street Institute of Child Health, University College London, London, UK
2. Craniofacial Development and Stem Cell Biology, Dental Institute, King's College London, London, UK
3. Institute of Human Genetics, Tumor Genetics Group, University of Göttingen, Germany
4. Department of Internal Medicine III, Technische Universität Dresden, Dresden, Germany

* Corresponding author: j.martinez-barbera@ucl.ac.uk

J.M.G.M current address: Basic Research Department, National Institute of Geriatrics, Blvd. Adolfo Ruiz Cortines 2767, Mexico City, P.C.10200, Mexico

Key words: Pituitary, development, mouse, sonic hedgehog, patched

SUMMARY STATEMENT

Using genetic approaches, we reveal that during normal murine development the SHH pathway is first required for normal specification of Rathke's pouch embryonic precursors and subsequently to control their proliferation.

ABSTRACT

Sonic hedgehog (SHH) is an essential morphogenetic signal dictating cell fate decisions in several developing organs in mammals. *In vitro* data suggest that SHH is required to specify LHX3+/LHX4+ Rathke's pouch (RP) progenitor identity. However, *in vivo* studies have failed to reveal such a function, supporting instead, a critical role for SHH in promoting proliferation of these RP progenitors and for differentiation of pituitary cell types. Here, we have used a genetic approach to demonstrate that activation of the SHH pathway is necessary to induce LHX3+/LHX4+ RP identity in mouse embryos. First, we show that conditional deletion of *Shh* in the anterior hypothalamus results in a fully penetrant phenotype characterised by a complete arrest of RP development, with lack of *Lhx3/Lhx4* expression in RP epithelium at 9.0 dpc (days post coitum) and total loss of pituitary tissue by 12.5 dpc. Conversely, over-activation of the SHH pathway by conditional deletion of *Ptch1* in RP progenitors leads to severe hyperplasia and enlargement of the Sox2+ve stem cell compartment by the end of gestation.

INTRODUCTION

Together, the pituitary gland and hypothalamus serve as the main regulator of the neuroendocrine axis, controlling critical physiological processes such as growth, reproduction, metabolism and stress response. The vertebrate pituitary is comprised of the anterior pituitary (AP), including the anterior and intermediate lobes (AL and IL, respectively), and the posterior pituitary (PP). The AP derives from Rathke's pouch (RP), a dorsal elevation of the oral ectoderm near the boundary with the pharyngeal endoderm, whilst the PP is of neural origin and originates from a recess of the overlying hypothalamus, the presumptive infundibulum (Davis and Camper, 2007; Rizzoti, 2015; Takuma et al., 1998; Treier et al., 1998). Progenitors in the periluminal epithelium of RP proliferate rapidly from 12.5 to 14.5 dpc, to subsequently exit the cell cycle and initiate cell-lineage commitment and differentiation into the different hormone-producing cells (Bilodeau et al., 2009; Davis et al., 2011). The AP contains six main hormone-secreting cell types: somatotrophs, (growth hormone, GH), lactotrophs, (prolactin, PRL), corticotrophs, (adrenocorticotropic hormone, ACTH), thyrotrophs, (thyroid stimulating hormone, TSH), gonadotrophs, (luteinising hormone, LH and follicle stimulating hormone, FSH) and melanotrophs (melanocyte-stimulating hormone, MSH). In addition, the AP contains Sox2+ve stem cells, which contribute to the postnatal expansion of the gland and organ homeostasis (Andoniadou et al., 2013; Rizzoti et al., 2013). The PP holds no endocrine cell types, but is instead richly endowed with axonal projections from hypothalamic neurons (Andersen & Rosenfeld, 2001; Castinetti et al, 2011; Kelberman et al., 2009). The function of the AP is primarily regulated by the parvocellular and magnocellular neurons, which reside in distinct nuclei in the hypothalamus (Andersen and Rosenfeld, 2001; Burbridge et al., 2016; Shimogori et al., 2010).

RP development is thought to be a step-wise process that requires at least two sequential inductive signals from the diencephalon (Takuma et al., 1998). First, BMP4 is required for induction and formation of a pouch rudiment and second, FGF8 signalling is necessary for activation of *Lhx3* and subsequent development of the pouch rudiment into a definitive RP (Takuma et al., 1998). Indeed, genetic evidence suggests that the acquisition of RP progenitor identity depends on the activation of *Lhx3* and *Lhx4* in the pouch rudiment epithelium at 9.0 dpc (Sheng et al., 1996; Sheng et al., 1997). Embryos homozygous null for *Lhx3* and *Lhx4* show early RP developmental arrest, where

only a rudimentary pouch is formed. No pituitary tissue is recognisable beyond 15.5 dpc, possibly due to decreased proliferation (Sheng et al., 1997) and/or increased apoptosis (Ellsworth et al., 2008; Raetzman et al., 2002; Zhao et al., 2006). Furthermore, double homozygous null embryos for *Pitx1* and *Pitx2*, two transcription factors expressed in the oral ectoderm and RP at 9.0 dpc, fail to activate *Lhx3/Lhx4* expression, resulting in severe RP developmental arrest (Charles et al., 2005; Suh et al., 2002).

Several *in vitro* and *in vivo* studies have established a critical role for hypothalamic expression of BMP4 and FGFs for activation of *Lhx3/Lhx4* expression in RP epithelium (Davis and Camper, 2007; Ericson et al., 1998a; Gleiberman et al., 1999; Norlin et al., 2000; Ohuchi et al., 2000; Ozone et al., 2016; Revest et al., 2001; Sbrogna et al., 2003; Suga et al., 2011; Takuma et al., 1998; Treier et al., 1998; Treier et al., 2001). In contrast, definitive *in vivo* evidence for a similar role of SHH is lacking. Genetic experiments in zebrafish and mouse have provided evidence supporting a role for Hedgehog signalling in the proliferation of LHX3+ve/LHX4+ve RP progenitors rather than in the initial induction of RP identity (i.e. activation of *Lhx3* and *Lhx4* expression) (Dutta et al., 2005; Herzog et al., 2003; Karlstrom et al., 1999; Park et al., 2000; Treier et al., 2001; Wang et al., 2010). Over-expression of the SHH inhibitor *Hhip* under the control the *Pitx1* promoter does not prevent the activation of *Lhx3/Lhx4* or formation of a definitive RP, but results in pituitary hypoplasia (Treier et al., 1998). Conversely, over-expression of *Shh* leads to pituitary hyperplasia, suggesting a proliferative role for SHH on already specified LHX3+ve/LHX4+ve RP progenitors. More recently, the anterior hypothalamic expression of *Shh* has been conditionally deleted using a specific SOX2-binding enhancer-Cre (*SBE2-Cre*) (Zhao et al., 2012). This leads to mis-patterning of the hypothalamus and RP hypoplasia, but *Lhx3/Lhx4* expression occurs in RP epithelium. In fact, in some embryos, multiple LHX3+ve/LHX4+ve pouches were observed. Genetic ablation in mice supports a critical role of *Gli* factors during hypothalamo-pituitary development but the exact mechanisms are still not fully clarified (Park et al., 2000; Wang et al., 2010).

In this manuscript, we have used genetic approaches in mouse to demonstrate that, in addition to promoting RP progenitor proliferation, hypothalamic *Shh* expression is essential for the initial activation of *Lhx3/Lhx4* transcription in RP epithelium and formation of a definitive pouch. In addition, we show that the anterior hypothalamus fails to differentiate.

RESULTS

The SHH pathway is active throughout normal pituitary development in mice and humans

First, we performed a detailed study to assess the expression of *Shh*/SHH and its effector target genes *Gli1* and *Ptch1* throughout pituitary development in both mice and humans.

At 9.5 and 10.5 dpc, *Shh* transcripts were detected within a rostral neural domain, including the developing anterior hypothalamus and ventral telencephalon, and a caudal domain, encompassing the posterior hypothalamus, possibly the mammillary area, and adjacent floorplate of the midbrain. There is a *Shh*-negative area between the mammillary region and anterior hypothalamus, likely corresponding to the tuberal hypothalamus (**Fig. 1 A,B**). At these stages, *Shh* expression was also observed in the pharyngeal endoderm immediately posterior to the developing RP, which was devoid of any *Shh* expression (**Fig. 1 A,B**). Although *Shh* expression was initially reported to be expressed in the oral ectoderm of wild-type embryos at 9.5-10.5 dpc (Treier et al., 1998; Treier et al., 2001), we could not detect the presence of *Shh* transcripts in this layer medially between 9.5 and 10.5 dpc, in agreement with a recent report (Zhao et al., 2012). To clarify further this discrepancy and assess the timing of *Shh* expression in the oral ectoderm, we performed a detailed expression analysis on histological sections of wildtype embryos from 16-46 somites (i.e. 9.0 to 11.5 dpc; (Hogan et al., 1994) (**Fig. S1**). By staging the embryos by somite number, we aimed to accurately pin-point the onset of *Shh* expression in this tissue. This study revealed that *Shh* mRNA is first detected in the lateral oral ectoderm adjacent to the developing RP in 33 somite-stage embryos (10.0 dpc) (**Fig. S1E″**). Strong expression in the lateral oral ectoderm was more evident at 42 and 46 somites (11-11.5

dpc) (**Fig. S1G″,H-H″).** RNAScope *in situ* hybridisation, enabling sensitive detection of mRNA expression up to single molecule resolution, confirmed the absence of *Shh* expression in the oral ectoderm at 16 somites (**Fig. S1A-A″**) (Wang et al., 2012).

Supporting the RNA expression pattern, SHH was strongly detected in the anterior hypothalamus, pharyngeal endoderm and a weak but consistent signal was also observed in the oral ectoderm and anterior part of RP epithelium, suggesting potential spreading of SHH from the pre-optic area towards the developing RP (**Fig. 1 G,H)**. From 11.5 to 14.5 dpc, *Shh* transcripts were detected within the developing hypothalamus (**Fig. 1C-E,I-K**) and by 18.5 dpc, signal was restricted to the ventricular zone of the 3rd ventricle (**Fig. 1F**). No obvious expression was detected in the developing pituitary by digoxigenin-labelled *Shh* riboprobes from 9.5-18.5 dpc (**Fig. 1F**). In contrast, SHH protein was clearly observed in single cells within the anterior pituitary at 18.5 dpc (**Fig. 1L**). In agreement with this, *Shh* transcripts were detected in sporadic single cells within the anterior pituitary at 18.5 dpc by RNAscope *in situ* hybridisation (**Supp. Fig. 2A,B**).

To assess the activation of the SHH pathway, the expression of the target genes *Gli1* and *Ptch1* was analysed by *in situ* hybridisation. At 9.5 dpc, *Gli1* transcripts were detected broadly throughout the developing hypothalamus and RP (**Fig. 1M**) and at 10.5 and 12.5 dpc, RP epithelium expressed *Gli1* robustly (**Fig. 1N-P**). By 14.5 dpc, *Gli1* transcripts were found mostly in the dorsal region of the periluminal epithelium of RP and by 18.5 dpc, expression was restricted to the marginal zone, a region of the anterior pituitary ventrally lining the cleft that is highly enriched for Sox2+ve stem cells (**Fig. 1Q,R**). However, in the hypothalamus, *Gli1* expression could not be detected in the ventral midline of the anterior hypothalamus or developing infundibulum from 10.5 dpc onwards, but signal was strong in the posterior hypothalamus, possibly including the prospective caudal tuberal and mammillary area (**Fig. 1N**). At 18.5 dpc, *Gli1* expression was restricted to the ventricular zone of the 3rd ventricle (**Fig. 1R**).

Ptch1 expression was also very dynamic. A 9.5 dpc, *Ptch1* transcripts were weakly detected in the posterior (forming mammillary region), strongly detected in the anterior hypothalamus and barely detected in the tuberal hypothalamus - patterns that became even more pronounced by 10.5 dpc

(**Fig. 1S,T**). Strong *Ptch1* signal was detected in the hypothalamus from 11.5-14.5 dpc, except for the infundibulum, and by 18.5 dpc, the hypothalamic signal was mostly detected in the ventricular zone of the 3rd ventricle (**Fig. 1U-X**). Within the developing RP, *Ptch1* expression was detected broadly in the epithelial progenitors at 9.5 dpc, but became progressively restricted to the ventral areas of RP, adjacent to the oral epithelium and pharyngeal endoderm by 11.5 dpc (**Fig. 1S-U**). At 12.5 dpc, only a small region of the periluminal epithelium of RP was positive for *Ptch1* transcripts (**Fig. 1V**). Subsequently, at 14.5 and clearly at 18.5 dpc, *Ptch1* transcripts were observed only in the marginal zone (**Fig. 1 W,X**).

At Carnegie stage 15 (CS15) in human fetal embryos, *SHH* transcripts and protein were identified in the anterior hypothalamus and pharyngeal endoderm, but were absent from the developing RP, similar to the mouse (**Supp. Fig. 3A-D**). *GLI1* transcripts were observed throughout the developing hypothalamus (**Supp. Fig. 3E,F**) and RP, suggesting activation of the pathway.

Together, these expression studies suggest that the SHH pathway is activated preferentially in regions containing undifferentiated precursors/stem cells, such as the RP periluminal epithelium at early stages of development and the marginal zone lining the cleft at 18.5 dpc. In addition, these analyses demonstrate the expression of SHH protein in tissues adjacent to the developing RP at early developmental stages, including the developing hypothalamus and pharyngeal endoderm suggesting that signalling from these domains may be required to activate the pathway in RP progenitors.

Deletion of *Shh* in the *Hesx1* cell lineage leads to pituitary aplasia in *Hesx1*$^{Cre/+}$;*Shh*$^{fl/-}$ mutants

The *Hesx1-Cre* mouse line drives Cre-mediated recombination in the anterior neural plate, including the prospective telencephalon and prospective anterior hypothalamus, as well as RP epithelium from 9.0 dpc (Jayakody et al., 2012). We generated *Hesx1*$^{Cre/+}$;*Shh*$^{fl/-}$ mice to study the consequences of early *Shh* deletion in the anterior hypothalamic area, as *Shh* is not expressed in RP epithelium and expression in the oral ectoderm occurs from 10.0 dpc.

Genotypic analysis of embryos between 9.5 and 18.5 dpc revealed no statistical deviation from the expected Mendelian ratios (**Table 1, n=361, Chi test p=0.9**). In contrast, genotyping of pups of up to 3 weeks of age, revealed a significant deviation from the expected ratios (**Table 1, n=67, Chi test p<0.001**). No *Hesx1*$^{Cre/+}$;*Shh*$^{fl/-}$ mice were identified postnatally, suggesting perinatal lethality.

Hesx1$^{Cre/+}$;*Shh*$^{fl/-}$ mutant embryos showed mild forebrain defects from 10.5 dpc, including a reduction in the size of the telencephalic vesicles, and by 11.5 dpc, loss of pigmented retina (**Fig. S4A-C**). A very small proportion of the mutant embryos showed more severe defects, including holoprosencephaly at 10.5 dpc (**n=4 out of 28**, **Fig. S4D-F)**. At 18.5 dpc, severe craniofacial defects as well as telencephalic and hypothalamic abnormalities were observed in all mutants analysed (**n=3, Fig. S5A-H)**. Pituitary tissue could not be identified morphologically at this stage in serial section analysis of the mutants (**Fig. S5I-L**).

Immunostaining against GH and PIT1, which label most of the pituitary cells at 18.5 dpc, revealed the complete lack of expression in serial sections in *Hesx1*$^{Cre/+}$;*Shh*$^{fl/-}$ mutants at 18.5 dpc (**Fig. S6)**. To further characterise the observed pituitary aplasia, we analysed embryos from 9.5 dpc onwards by haematoxylin-eosin staining. At 9.5 dpc, control embryos showed a close association between the evaginating RP epithelium and the floor of the neuroepithelium of the prospective infundibular area (**Fig. 2A**). In contrast, this intimate association was often lost in *Hesx1*$^{Cre/+}$;*Shh*$^{fl/-}$ mutant embryos and mesenchymal tissue was observed intercalated between RP and the neural epithelium and appeared to be over-grown (**Fig. 2B**). Reduced size and failure to contact the infundibular area was more obvious at 10.5 dpc and by 11.5 dpc, RP was severely hypoplastic and no infundibulum could be observed (**Fig. 2 C-F**). At 12.5 dpc, *Hesx1*$^{Cre/+}$;*Shh*$^{fl/-}$ mutant embryos displayed a fully penetrant phenotype in which RP was completely lost and no pituitary tissue could be identified from 12.5-18.5 dpc either by H&E or immunostaining (**Fig. 2G,H, Fig. S5**). RNA *in situ* hybridisation on serial histological sections of *Hesx1*$^{Cre/+}$;*Shh*$^{fl/-}$ mutants at 18.5 dpc revealed the loss or severe reduction in expression of most of the hypothalamic factors controlling pituitary function, including *Ghrh* (growth hormone-releasing hormone), *Ss* (somatostatin), *Ot* (oxytocin), *Avp* (arginine

vasopressin) and *Gnrh* (gonadotropin-releasing hormone) as well as *Pomc1* (proopiomelanocortin-alpha), suggesting loss of neuronal differentiation (**Fig. 3**).

The genetic deletion of *Shh* in the *Hesx1* cell lineage was assessed by RNA *in situ* hybridisation and immunofluorescence on histological sections of *Hesx1*$^{Cre/+}$;*Shh*$^{fl/-}$ and control littermates at 9.5 to 10.5 dpc. While in the control embryos, *Shh* transcripts were observed in the anterior and posterior developing hypothalamus, no *Shh* expression was detectable in the anterior hypothalamus in *Hesx1*$^{Cre/+}$;*Shh*$^{fl/-}$ mutants, despite the strong signal in the posterior hypothalamic area (**Fig. 4A-F)**. At 10.5 dpc, *Shh* expression was not detected within the developing RP in control embryos, however, a weak but consistent signal was detected in the posterior region of the evaginating RP in *Hesx1*$^{Cre/+}$;*Shh*$^{fl/-}$ mutants, that can be interpreted as a rostral extension of the pharyngeal endoderm *Shh* expression domain into the developing RP (**Fig. 4E,F**). Loss of SHH in the anterior hypothalamus and ectopic SHH expression in the posterior RP were also confirmed at the protein level by specific immunofluorescence staining (**Fig. 4G,H**). In agreement with the deletion of *Shh*, expression of *Ptch1* was lost in the anterior, yet present in the posterior hypothalamus in *Hesx1*$^{Cre/+}$;*Shh*$^{fl/-}$ mutants (**Fig. 4K,L**). Loss of *Ptch1* and *Gli1* expression was also observed in the anterior region of the developing RP, with transcripts detectable only in the posterior RP (**Fig. 4I-L**). Expression of *Shh* was observed in the oral ectoderm of the *Hesx1*$^{Cre/+}$;*Shh*$^{fl/-}$ mutants at 11.5 dpc, invading the epithelium of a rudimentary RP (**Fig. 4M,N**). These results demonstrate that, in addition to severe hypothalamic, telencephalic and craniofacial defects at late gestation, the early loss of *Shh* expression in the anterior hypothalamus results in abnormal development of RP from 9.5 dpc with pituitary aplasia from 12.5 dpc.

Anterior hypothalamus marker expression is lost in in *Hesx1*$^{Cre/+}$;*Shh*$^{fl/-}$ mutants

Fgf8 and *Bmp4* are essential signals controlling hypothalamus and RP development (Davis and Camper, 2007; Ericson et al., 1998). Transcripts for these secreted factors were normally expressed in the posterior hypothalamus at 10.5 dpc, which includes the tuberal hypothalamus and primordium of the infundibulum, but their expression domains do not reach the anterior hypothalamic area, where *Shh* is expressed (**Fig. 5A,C**). In contrast, the expression domains of these critical

hypothalamic signals were extended anteriorly in the *Hesx1*$^{Cre/+}$*;Shh*$^{fl/-}$ mutants, invading the domain where *Shh* was detected in the control embryos (**Fig. 5B,D**). The expression domains of *Tbx2* and *Tbx3*, two negative regulators of *Shh* expression (Trowe et al., 2013), were similar between *Hesx1*$^{Cre/+}$*;Shh*$^{fl/-}$ mutants and controls, although *Tbx3* expression domain appeared slightly expanded (**Fig. 5E-H**). *Nkx2.1*, another critical regulator of hypothalamic development (Kimura et al., 1996; Takuma et al., 1998), was broadly expressed throughout the hypothalamus in control embryos, but its expression domain was shortened in *Hesx1*$^{Cre/+}$*;Shh*$^{fl/-}$ mutants with a lack of expression in the anterior hypothalamus (**Fig. 5I,J**). *Otx2* is an important transcription factor required for normal development of the hypothalamus and pituitary (Acampora et al., 1995; Mortensen et al., 2015; Tajima et al., 2009). Immunostaining revealed OTX2 expression in the posterior hypothalamus, with a sharp boundary at the level where the infundibulum will develop, and the developing ventral telencephalon, with a negative region encompassing the anterior hypothalamus (**Fig. 5Q**). In contrast, in the *Hesx1*$^{Cre/+}$*;Shh*$^{fl/-}$ mutants OTX2 domain was broadly observed throughout the hypothalamus with no detectable negative area in the neuroepithelium, suggesting that the anterior hypothalamus was missing (**Fig. 5R**). Expression analysis with other regional markers including TCF4, Islet1 and *Wnt5a* as well as *Pomc1,* a marker of arcuate neurons, further demonstrated the loss of the anterior hypothalamus in *Hesx1*$^{Cre/+}$*;Shh*$^{fl/-}$ mutants (**Fig. 5K-P,S-X**). Loss of ACTH and TPIT neural expression was observed in the anterior hypothalamus of the mutants at 12.5 dpc (**Fig. S7**). Together, these analyses indicate a loss of expression of anterior hypothalamic markers concomitant with the rostral expansion of the expression domain of posterior hypothalamic markers in *Hesx1*$^{Cre/+}$*;Shh*$^{fl/-}$ mutants.

Loss of *Lhx3* and *Lhx4* expression in RP epithelium in *Hesx1*$^{Cre/+}$*;Shh*$^{fl/-}$ mutants

Embryos homozygous null for *Lhx3* and *Lhx4* show arrested RP development with absence of pituitary tissue by 15.5 dpc (Sheng et al., 1997), a phenotype very similar to that in *Hesx1*$^{Cre/+}$*;Shh*$^{fl/-}$ mutants. Indeed, neither *Lhx3* nor *Lhx4* expression were detected in RP in *Hesx1*$^{Cre/+}$*;Shh*$^{fl/-}$ mutants, either by *in situ* hybridisation or immunostaining from 9.0 dpc (16 somites) to 11.5 dpc (**Fig. 6A-D,G,H,K,L,M-P)**. Despite the failure to activate *Lhx3* and *Lhx4* expression, other RP markers such as

PITX1, SOX2, *Pitx2*, *Pax6*, *Six3*, Islet1 and *Wnt4* were found to be expressed in the developing RP in *Hesx1*$^{Cre/+}$*;Shh*$^{fl/-}$ mutants with no apparent differences compared to control embryos (**Fig. 6E,F,I,J,Q-X and Fig. 4S,T,W,X**).

The loss of pituitary tissue in *Lhx3*$^{-/-}$*;Lhx4*$^{-/-}$ double mutants has been attributed to decreased proliferation and/or increased apoptosis of RP progenitors. Immunostaining against activated Caspase-3, a marker of apoptotic cells (Wolf et al., 1999), revealed the presence of only a few scattered positive cells in RP at 11.5 dpc, and none at 9.5 or 10.5 dpc (**Fig. 7H-M**). A small but significant decrease in the mitotic index, as assessed using the mitotic marker phospho-histone H3 (Hendzel et al., 1997), was observed in *Hesx1*$^{Cre/+}$*;Shh*$^{fl/-}$ mutants at 11.5 dpc (**Fig. 7A-G**). Of note, comparable values were observed between mutants and control embryos at 9.5 and 10.5 dpc, suggesting that decreased proliferation may not be the only mechanism accounting for the pituitary aplasia observed in the *Hesx1*$^{Cre/+}$*;Shh*$^{fl/-}$ mutants from 12.5 dpc.

Hypothalamic BMP4 and FGF8 signals are important to induce LHX3+ve/LHX4+ve RP progenitor identity (Treier et al., 1998; Treier et al., 2001). As shown in **Fig. 5A-D**, the hypothalamic expression domains of these factors were anteriorised in *Hesx1*$^{Cre/+}$*;Shh*$^{fl/-}$ mutants at 10.5 dpc, a phenotype usually associated with increased recruitment of additional oral ectoderm into RP epithelium leading to RP enlargement or even the induction of multiple LHX3+/LHX4+ pouches (Dasen et al., 2001; Davis and Camper, 2007; Gaston-Massuet et al., 2016; Zhao et al., 2012). Therefore, it was interesting that even in the presence of more FGF and BMP signalling, RP development still arrested. Activation of the BMP and FGF pathways was demonstrated by the expression of p-SMAD1/5/8 and p-ERK1/2 in RP epithelium in *Hesx1*$^{Cre/+}$*;Shh*$^{fl/-}$ mutants and control embryos at 10.5 dpc, respectively (**Fig. S8C,D,G,H**). In addition, Sprouty2 (*Spry2*), a target gene of the FGF pathway (Minowada et al., 1999; Tefft et al., 1999), was expressed in the mutant RP at this stage, suggesting pathway activation (**Fig. S8A,B**). Expression of *Fgfr2*, which mediates FGF8 and FGF10 signalling (Turner and Grose, 2010), was also detected in the mutant RP (**Fig. S8A,B**). These results suggest that both the FGF and BMP signalling pathways are activated in the *Hesx1*$^{Cre/+}$*;Shh*$^{fl/-}$ mutant RP, excluding the possibility that the lack of *Lhx3* and *Lhx4* expression is due to the inability of RP epithelium to respond to these signals. In addition, these analyses demonstrate that the FGF and

BMP pathways are not sufficient to induce LHX3+ve/LHX4+ve RP identity in the absence of SHH signalling.

A change of fate of RP epithelium into oral ectoderm and pharyngeal endoderm contributes to the loss of pituitary tissue in *Hesx1$^{Cre/+}$;Shh$^{fl/-}$* mutants

We observed that markers normally expressed in either the oral ectoderm or pharyngeal endoderm, abutting the developing RP, were ectopically expressed and invaded the epithelium of the evaginating mutant RP. For example, *Bmp4* expression was detected in the oral epithelium but did not invade the anterior region of RP in control embryos at 10.5 dpc (**Fig. 5C**). However, ectopic *Bmp4* expression was consistently observed in the anterior region of RP in *Hesx1$^{Cre/+}$;Shh$^{fl/-}$* mutants, suggesting a caudal extension of the *Bmp4*+ve oral ectoderm into the developing pouch (**Fig. 5D**). Likewise, the expression of TCF4 (**Fig. 5O)** and SHH (**Fig. 4E,G)** was detected in the pharyngeal endoderm, but not in RP in control embryos at 10.5 dpc. In contrast, an anterior expansion of both TCF4 and SHH expression domain was observed in the *Hesx1$^{Cre/+}$;Shh$^{fl/-}$* mutants, with strong signal detectable in the posterior region of RP adjacent to the pharyngeal endoderm (**Fig. 5P, Fig. 4F, H**). Finally, these observations were further corroborated with other markers, such as N- and E-cadherin. In normal embryos at 10.5 dpc, E-cadherin is expressed in the oral ectoderm, pharyngeal endoderm but not in RP, which expresses N-cadherin (**Fig. 5U**). Anterior N-cadherin expression was lost in the *Hesx1$^{Cre/+}$;Shh$^{fl/-}$* mutant RP, which expressed E-cadherin (**Fig. 5V**). Similar ectopic expression was also revealed by immunostaining against Islet1, which was only identified in the ventral region of RP in control embryos, but throughout RP in *Hesx1$^{Cre/+}$;Shh$^{fl/-}$* mutants (**Fig. 5S,T**).

To further characterise the loss of RP progenitor identity, we performed gene expression analysis by RNA sequencing of manually dissected RP from *Hesx1$^{Cre/+}$;Shh$^{fl/-}$* mutant and control embryos at 10.5 dpc (n=2 RP per genotype). This study revealed a total of 208 significant differentially expressed genes between genotypes (adjusted p-value <0.1; **Fig. S9A**). Gene ontology analysis presented the term GO: 0029183 “Pituitary gland development” as a term significantly associated to these dysregulated genes (adjusted p-value <0.05; **Table S1**). Heatmap representation of expression levels of 12 genes involved in normal pituitary development revealed a significant down-

regulation of *Lhx3*, *Lhx4*, *Hesx1, Prop1* and *Six3* expression in the mutant relative to the control RP (**Fig. S9B; Table S2**). Furthermore, gene set enrichment analysis revealed a negative enrichment of genes associated with an active SHH pathway in the mutant relative to control RP (normalised enrichment score, NES = -1.73, false discovery rate, FDR = 0.008), demonstrating a down-regulation of the pathway in the *Hesx1*$^{Cre/+}$*;Shh*$^{fl/-}$ mutant RP, also supported by the Heatmap representation of SHH pathway genes (**Fig. S9C,D**). *Shh* mRNA was found to be non-significantly down-regulated in the *Hesx1*$^{Cre/+}$*;Shh*$^{fl/-}$ mutant RP (2.57 fold change, adjusted p-value 0.236), possibly reflecting the Cre-mediated deletion of the *Shh* locus.

Together, these analyses strongly suggest that the loss of *Shh* expression in the anterior hypothalamus results in failure to activate the SHH pathway and to initiate *Lhx3/Lhx4* expression in the RP epithelium. This may result in a progressive cell fate transformation of RP epithelium, whereby the rostral part of RP acquires a non-RP oral ectoderm fate whilst its posterior aspect turns into pharyngeal endoderm by 12.5 dpc.

Conditional over-activation of the SHH pathway leads to severe pituitary hyperplasia but normal differentiation of hormone-producing cells in *Hesx1*$^{Cre/+}$*;Ptch1*$^{fl/fl}$ mutants

We sought to explore the consequences of over-activating the pathway during hypothalamic-pituitary axis development by genetically deleting *Ptch1* in the *Hesx1*-cell lineage in *Hesx1*$^{Cre/+}$*;Ptch1*$^{fl/fl}$ mice.

Hesx1$^{Cre/+}$*;Ptch1*$^{fl/fl}$ mice die perinatally (**Table 2**) with severe forebrain and craniofacial defects (**Fig. S10**). Haematoxylin-eosin staining revealed no gross morphological defects in the developing RP or infundibulum between *Hesx1*$^{Cre/+}$*;Ptch1*$^{fl/fl}$ mutants and control embryos at 10.5 dpc (**Fig. 8A,B)**. The first clear evidence of a morphological defect was observed at 12.5 dpc (**Fig. 8C,D**), when the developing anterior lobe appeared hyperplastic in *Hesx1*$^{Cre/+}$*;Ptch1*$^{fl/fl}$ mutants compared with controls. Pituitary hyperplasia was more evident at 14.5 and 18.5 dpc, with an enlargement of the cleft and thickening of the anterior lobe in mutants relative to controls (**Fig. 8E-H**). Up-regulation of the SHH pathway in RP was observed from 10.5 dpc (**Fig. 8I-P**. Cell counting of dissociated

pituitaries at 18.5 dpc showed a total of 98,333 ± 4% cells in the pituitary of the *Hesx1*$^{Cre/+}$*;Ptch1*$^{fl/fl}$ versus 48,600 ± 9.4% ($p<0.01$) in the controls, confirming the hyperplasia.

Quantitative analysis of mitotic cells, revealed a significant increase in the mitotic index in the periluminal progenitors lining RP at 12.5 and 14.5 dpc, and cells around the pituitary cleft at 18.5 dpc in the *Hesx1*$^{Cre/+}$*;Ptch1*$^{fl/fl}$ mutants relative to the controls (**Fig. S11**). Patterning of the developing hypothalamus and specification of RP at 10.5 dpc occurred normally in *Hesx1*$^{Cre/+}$*;Ptch1*$^{fl/fl}$ mutants compared with control embryos (**Fig. S12**). Likewise, cell commitment and differentiation of hormone-producing cells was not prevented in the *Hesx1*$^{Cre/+}$*;Ptch1*$^{fl/fl}$ mutants (**Fig. S13 and S14**).

Over-activation of the SHH pathway results in expansion of the Sox2+ve stem cell compartment in *Hesx1*$^{Cre/+}$*;Ptch1*$^{fl/fl}$ mutants

At 14.5 dpc, the expression pattern of SOX2 was comparable between genotypes (**Fig. 9A, B**). In contrast, SOX9 expression in the developing AL appeared elevated in the *Hesx1*$^{Cre/+}$*;Ptch1*$^{fl/fl}$ mutants compared with controls (**Fig. 9E,F)**. At 18.5 dpc, numbers of SOX2 and SOX9+ve cells were significantly increased in the anterior pituitary and marginal zone of *Hesx1*$^{Cre/+}$*;Ptch1*$^{fl/fl}$ embryos compared with controls (**Fig. 9C, D, G-I**). It has previously been shown that pituitary cells with clonogenic potential *in vitro* are contained within the SOX2+ve cell population (Andoniadou et al., 2012; Andoniadou et al., 2013; Vankelecom, 2010). Culture of dissociated cells in stem-cell promoting media revealed a significant increase in clonogenic potential of the *Hesx1*$^{Cre/+}$*;Ptch1*$^{fl/fl}$ mutant pituitaries compared with controls at 18.5 dpc, evidenced by a 7-fold increase in numbers of clonogenic cells (**Fig. 9J)**. Together, these studies demonstrate that the activation of the SHH pathway by *Ptch1* deletion in *Hesx1*$^{Cre/+}$*;Ptch1*$^{fl/fl}$ mutants results in increase proliferation of LHX3+ve/LHX4+ve RP progenitors resulting in anterior pituitary hyperplasia and enlargement of the stem cell compartment at 18.5 dpc.

DISCUSSION

The main finding in this paper is the demonstration that SHH signalling is essential for the specification of LHX3+ve;LHX4+ve RP progenitors *in vivo*. *In vitro*, both in explant cultures of prospective RP oral epithelium (Treier et al., 2001) as well as embryonic stem cell aggregates (Ozone et al., 2016; Suga et al., 2011), SHH signals or the activation of this pathway using smoothened agonists is required for the specification of LHX3+ve progenitors. However, genetic approaches have failed to unravel this function, perhaps because the inhibition of the SHH pathway in the developing pituitary was not achieved early enough (Treier et al., 2001) or the deletion of the *Shh* expression in the anterior hypothalamus was incomplete (Zhao et al., 2012). Here, we show that the loss of SHH expression in the anterior hypothalamus in *Hesx1*$^{Cre/+}$*;Shh*$^{fl/-}$ embryos leads to down-regulation of the pathway and failure to activate the expression of LHX3 and LHX4 in the rudimentary RP epithelium at 9.0 dpc (i.e. 16 somite stage). As a consequence, there is a severe developmental arrest, no formation of a definitive pouch and loss of pituitary tissue by 12.5 dpc, a phenotype resembling that of the *Lhx3*$^{-/-}$*;Lhx4*$^{-/-}$ double homozygous mutants (Sheng et al., 1996; Sheng et al., 1997). These morphological and molecular defects observed in *Hesx1*$^{Cre/+}$*;Shh*$^{fl/-}$ mutants are also present in mouse mutants with disrupted BMP and FGF signalling, either due to loss/reduction of *Bmp* and *Fgf* expression in the hypothalamus or defective competence of RP to respond to hypothalamic BMP and FGF signals (De Moerlooze et al., 2000; Kimura et al., 1996; Ohuchi et al., 2000; Takuma et al., 1998). Being required does not necessarily mean that SHH is sufficient to induce RP specification, as the expansion of hypothalamic *Shh* expression in *Nkx2.1*$^{-/-}$ mutants does not induce *Lhx3* or *Lhx4* expression in the evaginating RP in the absence of normal BMP and FGF signalling (**Fig. 10**). Of note, *Nkx2.1* is primarily required within the hypothalamus for normal RP development (Takuma et al., 1998). Therefore, BMP, FGF and SHH are all required to induce RP progenitor fate at 9.5 dpc and cannot replace each other.

Our results demonstrate that the anterior hypothalamic expression of *Shh* is essential for normal patterning of the hypothalamus and potentially, these hypothalamic defects (i.e. up-regulation of *Tbx2* and *Tbx3* and reduction of *Wnt5a* and *TCF4* expression) could contribute to the RP

phenotype. *Shh* is expressed in the anterior endoderm (prechordal plate) at neural plate stages where it plays a role in patterning the ventral midline and in the separation of the eye fields as well as the telencephalic vesicles (Xavier et al., 2016). In *Hesx1*$^{Cre/+}$*;Shh*$^{fl/-}$ mutants, holoprosencephaly is infrequent and cyclopia is not observed, suggesting that signalling from the anterior endoderm is not compromised in the vast majority of the embryos. Although speculative, the excess of mesenchyme observed between the oral ectoderm and the anterior hypothalamus may interfere with signalling between the neural and oral ectoderm or have stimulatory or inhibitory effects that could also contribute to the phenotype. The reasons underlying the excess of mesenchyme are not known, but this defect may be related to the mis-patterning of the anterior hypothalamus (loss of *Shh* and ectopic *Fgf8/10* and *Bmp4* expression). Although we cannot rule out a contribution of other dysregulated signals, the fact that *Gli1* and *Ptch1* expression in the developing RP is down-regulated in *Hesx1*$^{Cre/+}$*;Shh*$^{fl/-}$ mutants supports a direct role for the SHH pathway in RP specification.

The accompanying paper by Travis et al., provides further insights into the potential mechanism underlying the loss of anterior hypothalamic tissue in the absence of SHH signals. Inhibition of the SHH pathway using cyclopamine in chick embryos at HH10-13 (10-15 somites) results in failure to form the anterior hypothalamus (*Six3*+ve;*Fgf10*-ve neuroepithelium), and instead *Six3*+ve;*Fgf10*+ve progenitors stay in the tuberal region, which in chick, is expanded in thickness. This observation is very similar to our results in *Hesx1*$^{Cre/+}$*;Shh*$^{fl/-}$ mutants (*Fgf8* and *Fgf10* are co-expressed in the posterior hypothalamus in mice; **Fig. S15;** Treier et al., 1998; Treier et al., 2001) and compatible with the phenotype observed by Zhao et al., 2012 where it was proposed that anterior hypothalamic SHH expression is essential to maintain critical gene expression boundaries along the antero-posterior axis of the midline hypothalamus. In addition, in Travis et al., the inhibition of the SHH pathway by using cyclopamine results in failure to induce LHX3+ve RP progenitor identity, recapitulating our murine data and in agreement with experiments in zebrafish (Sbrogna et al., 2003).

Analyses of the *Ptch1*-deleted mutants support the idea that the SHH pathway promotes cell proliferation of LHX3+ve/LHX4+ve RP progenitors during pituitary development. Of note, we failed to identify increased proliferation at 11.5 dpc, suggesting that persistent proliferation of RP

progenitors becomes apparent at developmental stages when they begin to exit the cell cycle and initiate differentiation (i.e. beyond 13.5-14.5 dpc) (Bilodeau et al., 2009; Davis et al., 2011). The consequence of maintained proliferation in periluminal progenitors beyond 14.5 dpc is the expansion of differentiated pituitary cells as well as the Sox2+ve stem cells. This finding is in agreement with *in vitro* data reported recently (Pyczek et al., 2016).

In conclusion, our data support the mainstream role of the SHH pathway in the control of cell proliferation during pituitary development and in addition, have revealed an essential role for SHH in the specification of RP progenitors *in vivo*.

MATERIALS AND METHODS

Mice and human pituitaries

The *Hesx1*$^{Cre/+,}$ *Shh*$^{fl/fl}$ or *Ptch1*$^{fl/fl}$ mice have been described previously (Andoniadou et al., 2007; Uhmann et al., 2007). *Shh*$^{fl/fl}$ mice were obtained from the Jackson Laboratory (B6;129-Shhtm2Amc/J). All mouse experiments were performed with Home Office and local ethical approval. Human embryonic samples were provided by the Joint MRC/Wellcome Trust (099175/Z/12/Z) Human Developmental Biology Resource. For further details, supplementary Materials and Methods.

Histology and *in situ* hybridisation on histological sections

Histological sections were stained using Harris' haematoxylin for morphology as previously described (Andoniadou et al., 2011). *In situ* hybridisation was performed on paraffin-embedded histological sections as previously described (Sajedi et al., 2013). For further details, supplementary Materials and Methods.

Cell counting *in vivo*

Cell counts *in vivo* were performed in 4-6 non-consecutive histological sections immunostained with antibodies. pHH3, SOX2 and SOX9 expressing cells were calculated from the percentage of positively stained cells as a proportion of the total DAPI positive nuclei. A total of 1000-5000 DAPI

positive cells and 100-1000 marker-positive cells were counted for each genotype. Analysis of SOX2 and SOX9 positive cells was assessed through determining the relative proportion of marker-positive cells to total DAPI positive nuclei in a section. These proportions were then applied to average cell counts of dissociated pituitaries to determine an approximate absolute number of these cell populations in the pituitary.

Immunofluorescence and RNAScope *in situ* hybridisation

Section immunostaining was performed as previously described (Andoniadou et al., 2013). RNAScope *in situ* hybridisation was performed according to the manufacturer's protocol (Wang et al., 2012) with conditions adapted for mouse embryos (Lodge et al., 2016). Embryos were formalin-fixed prior to processing and histological sections were cut at 5μm thickness. The *Shh* mouse specific probe, reagents and equipment were obtained from Advanced Cell Diagnostics. For further details, supplementary Materials and Methods.

RNA sequencing of dissected Rathke's pouch epithelium

RP were manually dissected from mutant and control embryos at 10.5 dpc (n=2 for each genotype). RNA sequencing was performed at the Wellcome Trust Genomics Unit, Oxford University. The data have been deposited in ArrayExpress (EMBL-EBI, Hinxton), accession number: E-MTAB-5822. For further details, supplementary Materials and Methods.

Assessment of clonogenic potential

Clonogenic assays were performed on murine anterior pituitaries as previously described (Andoniadou et al., 2012; Andoniadou et al., 2013). For further details, supplementary Materials and Methods.

Statistics

Mendelian ratios were calculated using the chi-squared test. Clonogenic potential of 18.5 dpc pituitaries and total cells counts *in vivo* were evaluated using an un-paired t-test.

ACKNOWLEDGMENTS

We thank the Developmental Studies Hybridoma Bank (University of Iowa) and the National Hormone and Peptide Program (Harbor-University of California, Los Angeles Medical Center) for providing some of the antibodies used in this study. The human embryonic and fetal material was provided by the Joint Medical Research Council (MRC)/Wellcome Trust Human Developmental Biology Resource (www.hdbr.org) (Grant 099175/Z/12/Z). This work was supported by the Medical Research Council (MRC) (Grants MR/M000125/1 and MR/L016729/1), Great Ormond Street Hospital for Children Charity/Children with Cancer UK (GOSHCC/CWCUK) (Grant W1055) and by the National Institute for Health Research Biomedical Research Centre at Great Ormond Street Hospital for Children National Health Service Foundation Trust and University College London. G.C. was recipient of a Child Health Research Appeal Trust (CHRAT) PhD fellowship. J.P.M.-B. is a Great Ormond Street Hospital Children's Charity Principal Investigator.

COMPETING INTERESTS

The other authors declare no competing interests.

AUTHOR CONTRIBUTIONS

G.C designed and performed the experiments and wrote the paper. J.A. performed the bioinformatics analysis. L.P., S.H. and J.M.G.-M., genotyped mice, performed *in situ* hybridisation and immunostaining. E.L. performed the RNAScope *in situ* hybridisation. H.H. provided the *Ptch1-flox* mouse line. C.L.A. designed the experiments and overviewed the project. J.P.M.-B. designed the experiments, overviewed the project and wrote the paper.

FUNDING

Medical Research Council (MRC) (Grants MR/M000125/1 and MR/L016729/1).

National Institute for Health Research Biomedical Research Centre at Great Ormond Street Hospital for Children National Health Service Foundation Trust and University College London.

Great Ormond Street Hospital for Children Charity/Children with Cancer UK (GOSHCC/CWCUK) (Grant W1055)

REFERENCES

Acampora, D., Mazan, S., Lallemand, Y., Avantaggiato, V., Maury, M., Simeone, A. and Brûlet, P. (1995). Forebrain and midbrain regions are deleted in Otx2-/- mutants due to a defective anterior neuroectoderm specification during gastrulation. *Development* **121**, 3279–90.

Andersen, B. and Rosenfeld, M. G. (2001). POU domain factors in the neuroendocrine system: lessons from developmental biology provide insights into human disease. *Endocr. Rev.* **22**, 2–35.

Andoniadou, C. L., Signore, M., Sajedi, E., Gaston-Massuet, C., Kelberman, D., Burns, A. J., Itasaki, N., Dattani, M. and Martinez-Barbera, J. P. (2007). Lack of the murine homeobox gene Hesx1 leads to a posterior transformation of the anterior forebrain. *Development* **134**, 1499–1508.

Andoniadou, C. L., Signore, M., Young, R. M., Gaston-Massuet, C., Wilson, S. W., Fuchs, E. and Martinez-Barbera, J. P. (2011). HESX1- and TCF3-mediated repression of Wnt/ B-catenin targets is required for normal development of the anterior forebrain. *Development* **4942**, 4931–4942.

Andoniadou, C. L., Gaston-Massuet, C., Reddy, R., Schneider, R. P., Blasco, M. a, Le Tissier, P., Jacques, T. S., Pevny, L. H., Dattani, M. T., Martinez-Barbera, J. P., et al. (2012). Identification of novel pathways involved in the pathogenesis of human adamantinomatous craniopharyngioma. *Acta Neuropathol.*

Andoniadou, C. L., Matsushima, D., Mousavy-gharavy, S. N., Signore, M., Mackintosh, A. I., Schaeffer, M., Gaston-massuet, C., Mollard, P., Jacques, T. S., Tissier, P. Le, et al. (2013). The Sox2 + population of the adult murine pituitary includes progenitor / stem cells with tumour-inducing potential. *Cell Stem Cell*.

Bilodeau, S., Roussel-Gervais, A. and Drouin, J. (2009). Distinct developmental roles of cell cycle inhibitors p57Kip2 and p27Kip1 distinguish pituitary progenitor cell cycle exit from cell cycle reentry of differentiated cells. *Mol. Cell. Biol.* **29**, 1895–908.

Burbridge, S., Stewart, I. and Placzek, M. (2016). Development of the Neuroendocrine Hypothalamus. *Compr. Physiol.* **6**, 623–43.

Castinetti, F., Davis, S. W., Brue, T. and Camper, S. a (2011). Pituitary stem cell update and potential implications for treating hypopituitarism. *Endocr. Rev.* **32**, 453–471.

Charles, M. A., Suh, H., Hjalt, T. A., Drouin, J., Camper, S. A. and Gage, P. J. (2005). PITX genes are required for cell survival and Lhx3 activation. *Mol. Endocrinol.* **19**, 1893–903.

Dasen, J. S., Martinez Barbera, J. P., Herman, T. S., Connell, S. O., Olson, L., Ju, B., Tollkuhn, J., Baek, S. H., Rose, D. W. and Rosenfeld, M. G. (2001). Temporal regulation of a paired-like homeodomain repressor/TLE corepressor complex and a related activator is required for pituitary organogenesis. *Genes Dev.* **15**, 3193–207.

Davis, S. W. and Camper, S. a (2007). Noggin regulates Bmp4 activity during pituitary induction. *Dev. Biol.* **305**, 145–160.

Davis, S. W., Mortensen, A. H. and Camper, S. a (2011). Birthdating studies reshape models for pituitary gland cell specification. *Dev. Biol.* **352**, 215–227.

De Moerlooze, L., Spencer-Dene, B., Revest, J. M., Hajihosseini, M., Rosewell, I. and Dickson, C. (2000). An important role for the IIIb isoform of fibroblast growth factor receptor 2 (FGFR2) in mesenchymal-epithelial signalling during mouse organogenesis. *Development* **127**, 483–92.

Dutta, S., Dietrich, J.-E., Aspöck, G., Burdine, R. D., Schier, A., Westerfield, M. and Varga, Z. M. (2005). Pitx3 Defines an Equivalence Domain for Lens and Anterior Pituitary Placode. *Development* **132**, 1579–1590.

Ellsworth, B. S., Butts, D. L. and Camper, S. A. (2008). Mechanisms underlying pituitary hypoplasia and failed cell specification in Lhx3-deficient mice. *Dev. Biol.* **313**, 118–129.

Ericson, J., Norlin, S., Jessell, T. M. and Edlund, T. (1998). Integrated FGF and BMP signaling controls the progression of progenitor cell differentiation and the emergence of pattern in the embryonic anterior pituitary. *Development* **125**, 1005–15.

Gaston-Massuet, C., McCabe, M. J., Scagliotti, V., Young, R. M., Carreno, G., Gregory, L. C., Jayakody, S. A., Pozzi, S., Gualtieri, A., Basu, B., et al. (2016). Transcription factor 7-like 1 is involved in hypothalamo–pituitary axis development in mice and humans. *Proc. Natl. Acad. Sci.* **113**, E548–E557.

Gleiberman, a S., Fedtsova, N. G. and Rosenfeld, M. G. (1999). Tissue interactions in the induction of anterior pituitary: role of the ventral diencephalon, mesenchyme, and notochord. *Dev. Biol.* **213**, 340–353.

Hendzel, M. J., Wei, Y., Mancini, M. A., Van Hooser, A., Ranalli, T., Brinkley, B. R., Bazett-Jones, D. P. and Allis, C. D. (1997). Mitosis-specific phosphorylation of histone H3 initiates primarily within pericentromeric heterochromatin during G2 and spreads in an ordered fashion coincident with mitotic chromosome condensation. *Chromosoma* **106**, 348–60.

Herzog, W., Zeng, X., Lele, Z., Sonntag, C., Ting, J.-W., Chang, C.-Y. and Hammerschmidt, M. (2003). Adenohypophysis formation in the zebrafish and its dependence on sonic hedgehog. *Dev. Biol.* **254**, 36–49.

Hogan, B.L., R., B., Constantini, F., Lacy, E. (1994). Manipulating the mouse embryo, a laboratory manual. Cold Spring Harbor Laboratory Press second edition, pages 24-25.

Jayakody, S. A., Andoniadou, C. L., Gaston-massuet, C., Signore, M., Cariboni, A., Bouloux, P. M., Tissier, P. Le, Pevny, L. H., Dattani, M. T. and Martinez-barbera, J. P. (2012). SOX2 regulates the hypothalamic-pituitary axis at multiple levels. *J. Clin. Invest.* **122**, 3635–3646.

Karlstrom, R. O., Talbot, W. S. and Schier, A. F. (1999). Comparative synteny cloning of zebrafish you-too: mutations in the Hedgehog target gli2 affect ventral forebrain patterning. *Genes Dev.* **13**, 388–93.

Kelberman, D., Rizzoti, K., Lovell-Badge, R., Robinson, I. C. a F. and Dattani, M. T. (2009). Genetic regulation of pituitary gland development in human and mouse. *Endocr. Rev.* **30**, 790–829.

Kimura, S., Hara, Y., Pineau, T., Fernandez-Salguero, P., Fox, C. H., Ward, J. M. and Gonzalez, F. J. (1996). The T/ebp null mouse: thyroid-specific enhancer-binding protein is essential for the organogenesis of the thyroid, lung, ventral forebrain, and pituitary. *Genes Dev.* **10**, 60–9.

Lodge, E. J., Russell, J. P., Patist, A. L., Francis-West, P. and Andoniadou, C. L. (2016). Expression Analysis of the Hippo Cascade Indicates a Role in Pituitary Stem Cell Development. *Front. Physiol.* **7**, 114.

Minowada, G., Jarvis, L. A., Chi, C. L., Neubüser, A., Sun, X., Hacohen, N., Krasnow, M. A. and Martin, G. R. (1999). Vertebrate Sprouty genes are induced by FGF signaling and can cause chondrodysplasia when overexpressed. *Development* **126**, 4465–75.

Mortensen, A. H., Schade, V., Lamonerie, T. and Camper, S. A. (2015). Deletion of OTX2 in neural ectoderm delays anterior pituitary development. *Hum. Mol. Genet.* **24**, 939–53.

Norlin, S., Nordström, U. and Edlund, T. (2000). Fibroblast growth factor signaling is required for the proliferation and patterning of progenitor cells in the developing anterior pituitary. *Mech. Dev.* **96**, 175–182.

Ohuchi, H., Hori, Y., Yamasaki, M., Harada, H., Sekine, K., Kato, S. and Itoh, N. (2000). FGF10 Acts as a Major Ligand for FGF Receptor 2 IIIb in Mouse Multi-Organ Development. *Biochem. Biophys. Res. Commun.* **277**, 643–649.

Ozone, C., Suga, H., Eiraku, M., Kadoshima, T., Yonemura, S., Takata, N., Oiso, Y., Tsuji, T. and Sasai, Y. (2016). Functional anterior pituitary generated in self-organizing culture of human embryonic stem cells. *Nat. Commun.* **7**, 10351.

Park, H. L., Bai, C., Platt, K. A., Matise, M. P., Beeghly, A., Hui, C. C., Nakashima, M., Joyner, A. L., Alexandre, C., Jacinto, A., et al. (2000). Mouse Gli1 mutants are viable but have defects in SHH signaling in combination with a Gli2 mutation. *Development* **127**, 1593–605.

Pyczek, J., Buslei, R., Schult, D., Hölsken, A., Buchfelder, M., Heß, I., Hahn, H., Uhmann, A., Hooper, J. E., Scott, M. P., et al. (2016). Hedgehog signaling activation induces stem cell proliferation and hormone release in the adult pituitary gland. *Sci. Rep.* **6**, 24928.

Raetzman, L. T., Ward, R. and Camper, S. A. (2002). Lhx4 and Prop1 are required for cell survival and expansion of the pituitary primordia. *Development* **129**, 4229–39.

Revest, J.-M., Spencer-Dene, B., Kerr, K., De Moerlooze, L., Rosewell, I. and Dickson, C. (2001). Fibroblast Growth Factor Receptor 2-IIIb Acts Upstream of Shh and Fgf4 and Is Required for Limb Bud Maintenance but Not for the Induction of Fgf8, Fgf10, Msx1, or Bmp4. *Dev. Biol.* **231**, 47–62.

Rizzoti, K. (2015). Genetic regulation of murine pituitary development. *J. Mol. Endocrinol.* **54**, R55–73.

Rizzoti, K., Akiyama, H. and Lovell-Badge, R. (2013). Mobilized Adult Pituitary Stem Cells Contribute to Endocrine Regeneration in Response to Physiological Demand. *Cell Stem Cell* **13**, 419–432.

Sajedi, E., Gaston-Massuet, C., Signore, M., Andoniadou, C. L., Kelberman, D., Castro, S., Etchevers, H. C., Gerrelli, D., Dattani, M. T. and Martinez-Barbera, J. P. (2013). Analysis of mouse models carrying the I26T and R160C substitutions in the transcriptional repressor HESX1 as models for septo-optic dysplasia and hypopituitarism. *Dis. Model. Mech.* **1**, 241–254.

Sbrogna, J. L., Barresi, M. J. . and Karlstrom, R. O. (2003). Multiple roles for Hedgehog signaling in zebrafish pituitary development. *Dev. Biol.* **254**, 19–35.

Sheng, H. Z., Zhadanov, A. B., Mosinger, B., Fujii, T., Bertuzzi, S., Grinberg, A., Lee, E. J., Huang, S. P., Mahon, K. A., Westphal, H., et al. (1996). Specification of pituitary cell lineages by the LIM homeobox gene Lhx3. *Science* **272**, 1004–7.

Sheng, H. Z., Moriyama, K., Yamashita, T., Li, H., Potter, S. S., Mahon, K. A. and Westphal, H. (1997). Multistep control of pituitary organogenesis. *Science* **278**, 1809–12.

Shimogori, T., Lee, D. a, Miranda-Angulo, A., Yang, Y., Wang, H., Jiang, L., Yoshida, A. C., Kataoka, A., Mashiko, H., Avetisyan, M., et al. (2010). A genomic atlas of mouse hypothalamic development. *Nat. Neurosci.* **13**, 767–775.

Suga, H., Kadoshima, T., Minaguchi, M., Ohgushi, M., Soen, M., Nakano, T., Takata, N., Wataya, T., Muguruma, K., Miyoshi, H., et al. (2011). Self-formation of functional adenohypophysis in three-dimensional culture. *Nature* **480**, 57–62.

Suh, H., Gage, P. J., Drouin, J. and Camper, S. A. (2002). Pitx2 is required at multiple stages of pituitary organogenesis: pituitary primordium formation and cell specification. *Development* **129**, 329–37.

Tajima, T., Ohtake, A., Hoshino, M., Amemiya, S., Sasaki, N., Ishizu, K. and Fujieda, K. (2009). OTX2 Loss of Function Mutation Causes Anophthalmia and Combined Pituitary Hormone Deficiency with a Small Anterior and Ectopic Posterior Pituitary. *J. Clin. Endocrinol. Metab.* **94**, 314–319.

Takuma, N., Sheng, H. Z., Furuta, Y., Ward, J. M., Sharma, K., Hogan, B. L., Pfaff, S. L., Westphal, H., Kimura, S. and Mahon, K. A. (1998). Formation of Rathke's pouch requires dual induction from the diencephalon. *Development* **125**, 4835–40.

Tefft, J. D., Lee, M., Smith, S., Leinwand, M., Zhao, J., Bringas, P., Crowe, D. L. and Warburton, D. (1999). Conserved function of mSpry-2, a murine homolog of Drosophila sprouty, which negatively modulates respiratory organogenesis. *Curr. Biol.* **9**, 219–22.

Treier, M., Gleiberman, A. S., O'Connell, S. M., Szeto, D. P., McMahon, J. A., McMahon, A. P. and Rosenfeld, M. G. (1998). Multistep signaling requirements for pituitary organogenesis in vivo. *Genes Dev.* **12**, 1691–704.

Treier, M., O'Connell, S., Gleiberman, a, Price, J., Szeto, D. P., Burgess, R., Chuang, P. T., McMahon, a P. and Rosenfeld, M. G. (2001). Hedgehog signaling is required for pituitary gland development. *Development* **128**, 377–386.

Trowe, M.-O., Zhao, L., Weiss, A.-C., Christoffels, V., Epstein, D. J. and Kispert, A. (2013). Inhibition of Sox2-dependent activation of Shh in the ventral diencephalon by Tbx3 is required for formation of the neurohypophysis. *Development* **140**, 2299–2309.

Turner, N. and Grose, R. (2010). Fibroblast growth factor signalling: from development to cancer. *Nat. Rev. Cancer* **10**, 116–129.

Uhmann, A., Dittmann, K., Nitzki, F., Dressel, R., Koleva, M., Frommhold, A., Zibat, A., Binder, C., Adham, I., Nitsche, M., et al. (2007). The Hedgehog receptor Patched controls lymphoid lineage commitment. *Blood* **110**, 1814–23.

Vankelecom, H. (2010). Pituitary stem/progenitor cells: embryonic players in the adult gland? *Eur. J. Neurosci.* **32**, 2063–2081.

Xavier, G.M., Seppala, M., Barrell, W., Birjandi, A.A., Geoghegan, F., Cobourne, M.T. (2016). Hedgehog receptor function during craniofacial development. *Dev. Biol.* **415**, 198-215.

Wang, Y., Martin, J. F. and Bai, C. B. (2010). Direct and indirect requirements of Shh/Gli signaling in early pituitary development. *Dev. Biol.* **348**, 199–209.

Wang, F., Flanagan, J., Su, N., Wang, L.-C., Bui, S., Nielson, A., Wu, X., Vo, H.-T., Ma, X.-J. and Luo, Y. (2012). RNAscope: a novel in situ RNA analysis platform for formalin-fixed, paraffin-embedded tissues. *J. Mol. Diagn.* **14**, 22–9.

Wolf, B. B., Schuler, M., Echeverri, F. and Green, D. R. (1999). Caspase-3 is the primary activator of apoptotic DNA fragmentation via DNA fragmentation factor-45/inhibitor of caspase-activated DNase inactivation. *J. Biol. Chem.* **274**, 30651–6.

Zhao, Y., Morales, D. C., Hermesz, E., Lee, W.-K., Pfaff, S. L. and Westphal, H. (2006). Reduced expression of the LIM-homeobox gene Lhx3 impairs growth and differentiation of Rathke's pouch and increases cell apoptosis during mouse pituitary development. *Mech. Dev.* **123**, 605–613.

Zhao, L., Zevallos, S. E., Rizzoti, K., Jeong, Y., Lovell-Badge, R. and Epstein, D. J. (2012). Disruption of SoxB1-dependent Sonic hedgehog expression in the hypothalamus causes septo-optic dysplasia. *Dev. Cell* **22**, 585–96.

Figures

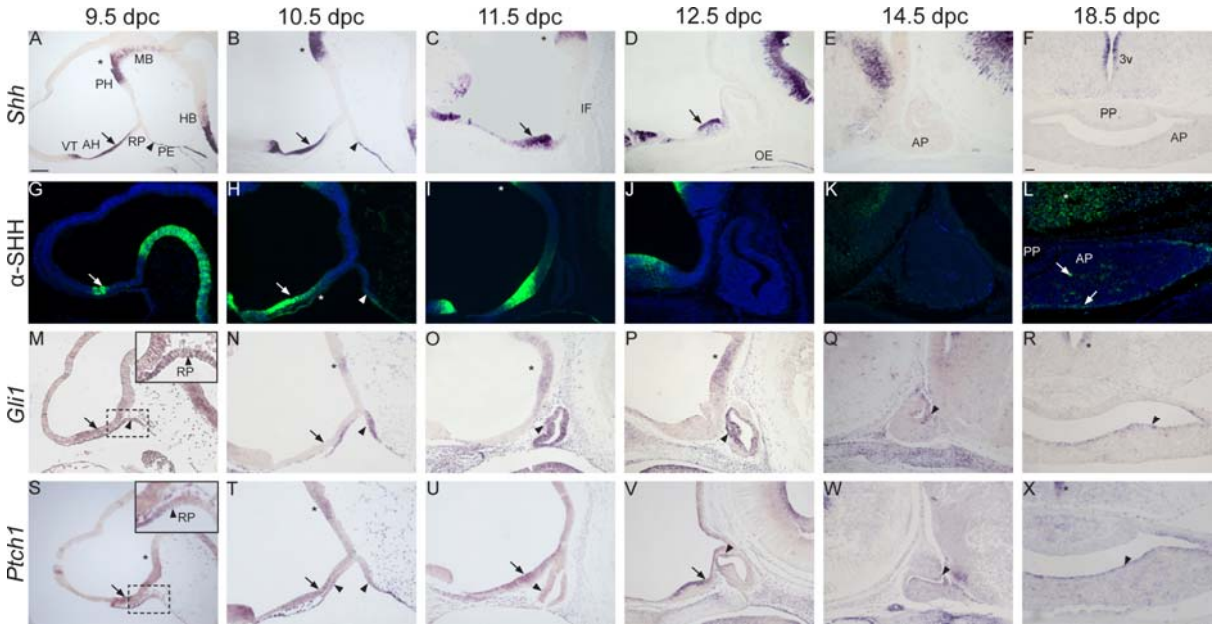

Fig. 1. Expression of *Shh*/SHH, *Gli1* and *Ptch1* during normal pituitary development. *In situ* hybridisation and immunofluorescence on wild-type mid-sagittal (A-E, G-K, M-Q, S-W) and frontal sections (F,L,R,X) during pituitary organogenesis between 9.5 and 18.5 dpc. (**A-F**) *Shh* transcripts are detected in the anterior hypothalamus (AH, arrows), posterior hypothalamus (PH, asterisks) and pharyngeal endoderm (PE, arrowhead) abutting the developing Rathke's pouch (RP). Note the expression in the subventricular zone around the 3rd ventricle (3v). (**G-L**) SHH immunostaining is observed in a similar pattern. Note the weak SHH signal in the anterior region of RP at 10.5 dpc (H, asterisk). Single SHH+ve cells are detected at 18.5 dpc in the AP (arrows) and overlying hypothalamus (asterisk in L). (**M-R**) *In situ* hybridisation against *Gli1*. Note that the expression of *Gli1* in the developing RP (M-O, arrowheads), periluminal epithelium (P,Q, arrowheads) and marginal zone of the anterior pituitary (R, arrowhead). Within the hypothalamus, *Gli1* transcripts are initially detected in the AH (M, arrow), but become restricted to the PH from 10.5 dpc (N-P, asterisks) and subventricular zone of the 3rd ventricle at 18.5 dpc (asterisk in R). (**S-X**) *Ptch1* transcripts are observed in the AH (arrows), PH (asterisks) and around the 3rd ventricle (asterisk in X).

Within RP, *Ptch1* is initially expressed in the rostral region of the evaginating RP at 9.5 dpc (arrowhead in the inset in S), at the boundary of RP with oral ectoderm and pharyngeal endoderm (arrowheads in T) and ventral region of the pinched-off pouch (arrowhead in U). Subsequently, *Ptch1* transcripts are localised within the periluminal epithelium and marginal zone (arrowheads in V-X). Abbreviations: RP, Rathke's pouch; PH, posterior hypothalamus; AH, anterior hypothalamus; AP, anterior pituitary; PP Posterior pituitary; IF, infundibulum; OE, oral endoderm; PE pharyngeal endoderm; 3v, third ventricle. Scale bar is 100μm.

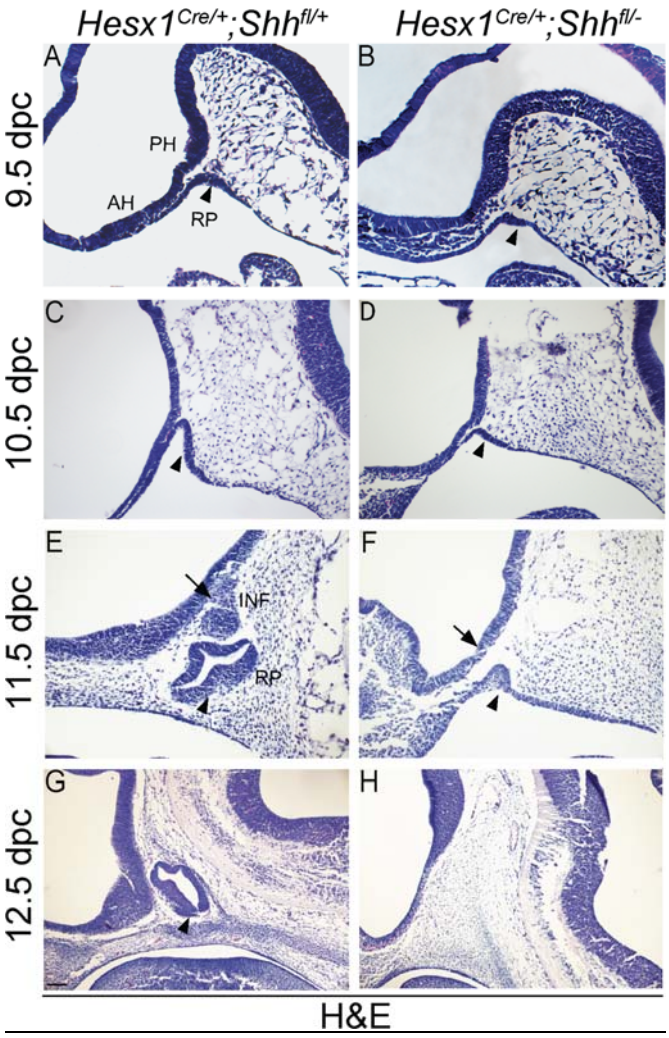

Fig. 2. Developmental arrest and loss of pituitary tissue in *Hesx1*$^{Cre/+}$;*Shh*$^{fl/-}$ mutants by 12.5 dpc. Haematoxylin and eosin (H&E) staining on mid-sagittal sections of *Hesx1*$^{Cre/+}$;*Shh*$^{fl/-}$ mutants and control embryos. (**A,B**) The evaginating RP (arrowheads) is observable in both genotypes at 9.5 dpc, but it looks smaller and not intimately associated to the overlying neural ectoderm in the mutant compared with the control embryo. (**C,D**) RP is clearly hypoplastic in the *Hesx1*$^{Cre/+}$;*Shh*$^{fl/-}$ mutant relative to the control embryo at 10.5 dpc (arrowheads). (**E-F**) The mutant RP is severely hypoplastic, has not detached form the oral ectoderm and does not make contact with the overlying hypothalamus compared with the control RP (arrowheads). Note the lack of infundibulum (INF, arrow in E) in the mutant embryo. (**G,H**) Note the complete loss of pituitary tissue in the mutant relative to the control embryo (arrowhead). Abbreviations as in Fig. 1. Scale bar is 100μm.

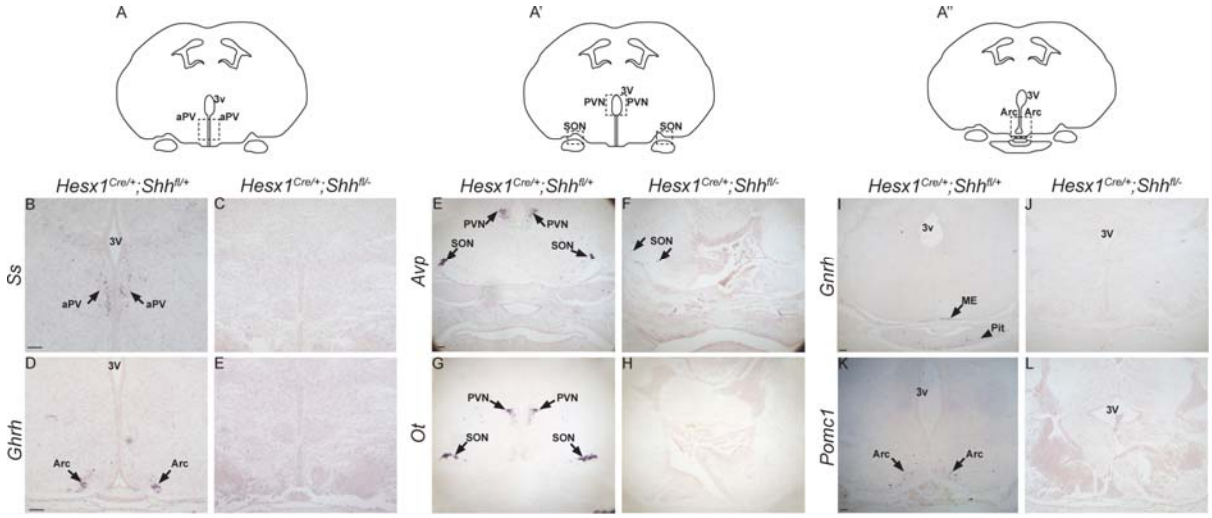

Fig. 3. Loss of expression of hypothalamic factors in *Hesx1$^{Cre/+}$;Shh$^{fl/-}$* mutants at 18.5 dpc. *In situ* hybridisation against the hypothalamic factors somatostatin (*Ss*), growth hormone-releasing hormone (*Ghrh*), gonadotrophin-releasing hormone (*Gnrh*), proopiomelanocortin (*Pomc1*), arginine-vassopressin (*Avp*) and *Oxytocin* (*Ot*) on frontal sections of *Hesx1$^{Cre/+}$;Shh$^{fl/-}$* and control embryos at 18.5 dpc. (**A**) Schematic representation of the plane of section indicating the positions of the anterior periventricular (aPV) and arcuate (arc) nuclei. (**B-I**) Note the loss of expression of *Ss*, *Ghrh*, *Gnrh* and *Pomc1* in the mutants. (**J**) Schematic representation of the plane of section showing the approximate location of the supraoptic (SON) and paraventricular (PVN) nuclei. (**K-N**) Note the severe reduction in *Avp* and absence of *Ot* expression in the mutants compared with the control embryos. Abbreviations: aPV, anterior periventricular nuclei; Arc, arcuate nuclei; PVN, paraventricular nuclei; SON, supraoptic nuclei; 3V, third ventricle. Scale bar: 100μm

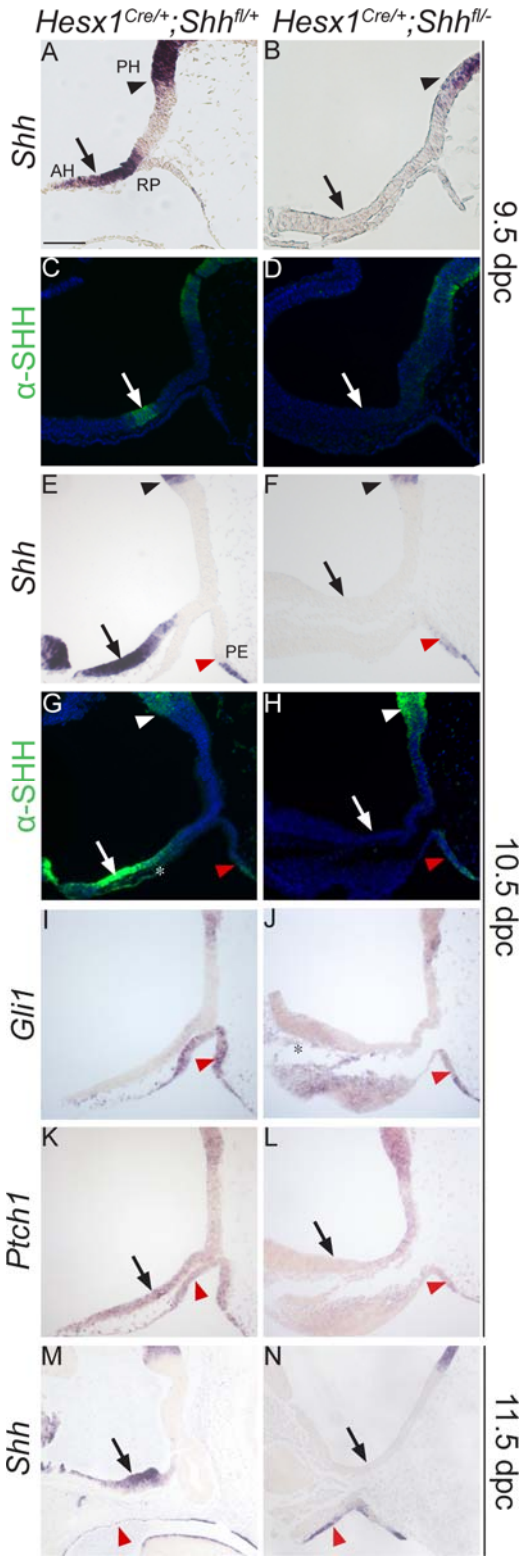

Fig. 4. Loss of *Shh* expression in the anterior hypothalamus of *Hesx1*$^{Cre/+}$;*Shh*$^{fl/-}$ mutants results in reduced *Gli1* and *Ptch1* expression in the developing Rathke's pouch. *In situ* hybridisation against *Shh* and anti-SHH immunofluorescent staining on mid-sagittal sections of control and

Hesx1$^{Cre/+}$;*Shh*$^{fl/-}$ mutant embryos at 9.5 and 10.5 dpc. (**A-G**) Expression of *Shh* transcripts (A,B,E,F) or SHH protein (C,D,G,H) is detected in the anterior and posterior hypothalamus in the control embryos, but is completely undetectable in the AH in the mutant embryos (AH, arrows and PH, arrowheads). *Shh*/SHH expression is not detected in the developing RP in the control embryos, but there is ectopic *Shh*/SHH signal in the posterior region of the developing RP adjacent to the pharyngeal endoderm (PE, red arrowhead) in the mutant RP. (**I,J**) *Gli1* transcripts are strongly detected in the control RP (arrowhead in I), but barely detectable and mostly restricted to the posterior region in the mutant RP (arrowhead in J). Note the Gli1 expression in head mesenchyme underlying the AH in the mutant (asterisk in J). (**K,L**) *Ptch1* expression is lost in the AH (arrow) and developing RP (arrowhead) in the mutant relative to the control embryo. (**M,N**) *Shh* transcripts are not detected in the anterior hypothalamus in the mutant embryo (arrows), but are detected throughout the oral ectoderm and pharyngeal endoderm in both the mutant and control embryos (arrowhead). Abbreviations as in Fig. 1. Scale bar is 100 μm.

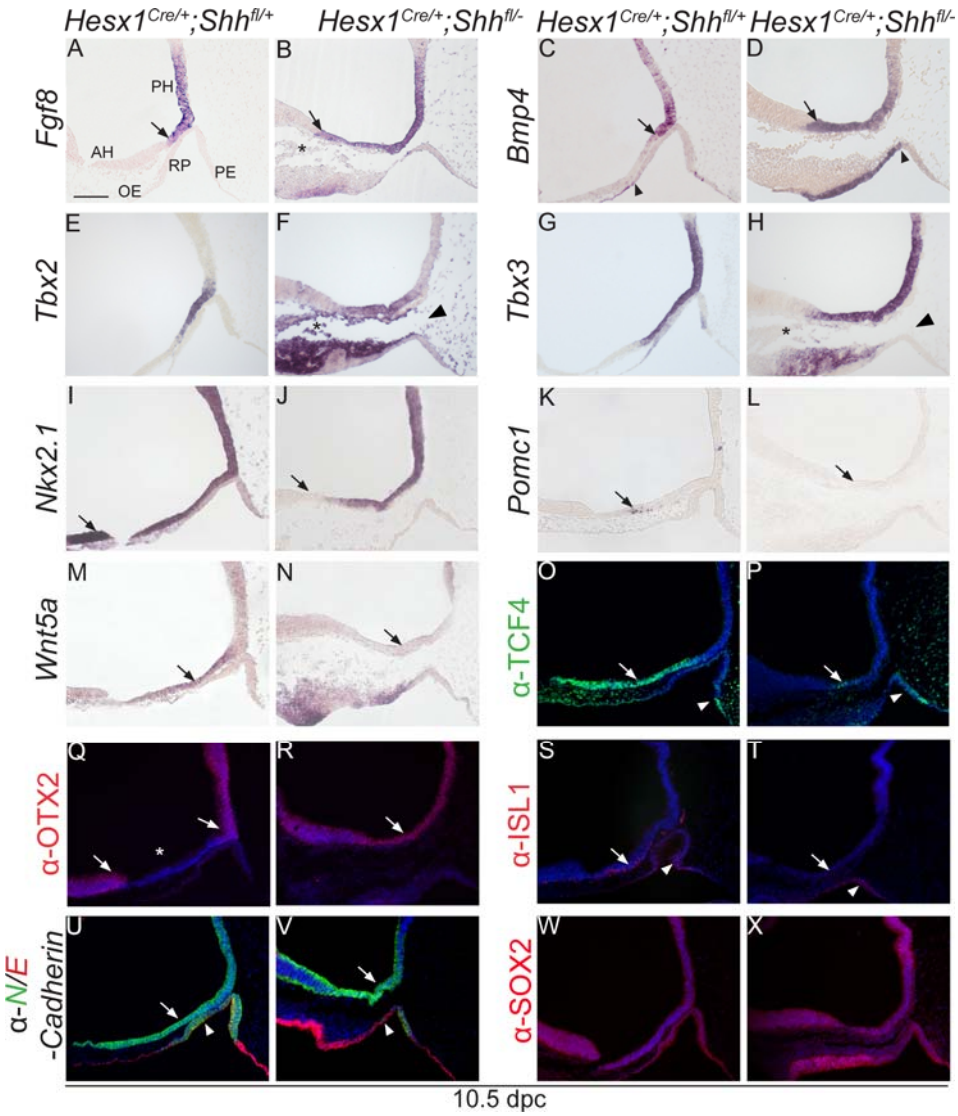

Fig. 5. Anterior hypothalamic identity is lost in *Hesx1*$^{Cre/+}$*;Shh*$^{fl/-}$ mutant embryos. *In situ* hybridisation and immunofluorescence on mid-sagittal sections at 10.5 dpc of control and *Hesx1*$^{Cre/+}$*;Shh*$^{fl/-}$ mutant embryos. (**A-D**) *Fgf8* and *Bmp4* expression domains are restricted to the posterior hypothalamus (PH) in the control embryos (arrow in A,C), but are remarkably anteriorised in the mutants (arrow in B,D). Note the ectopic expression of *Bmp4* in the anterior region of the mutant Rathke's pouch (RP) (arrowhead in D). (**E-H**) *Tbx2* and *Tbx3* transcripts are detected in the hypothalamus, in the region overlying RP (possibly the prospective infundibulum). Note the expression of these markers in the head mesenchyme underlying the hypothalamus (asterisk) and the separation between RP and the prospective infundibular area in the mutant embryo (arrowhead in F). (**I,J**) The expression domain of *Nkx2.1* is shorter in the mutant compare with the control embryo

(arrow). (**K,L**) *Pomc1* transcripts are lost in the mutant AH compared with the control (arrows). (**M,N**) The *Wnt5a* expression domain is reduced in the mutant AH compared with the control (arrows). (**O,P**) TCF4 is expressed in the AH in the control embryo, but its expression is markedly reduced in the mutant (arrows). Note the TCF4 ectopic expression in the posterior region of RP (arrowhead in P). (**Q,R**) In the control embryo (Q), immunostaining against OTX2 shows expression in the posterior hypothalamus (arrow) and ventral telencephalon (arrowhead), but no signal is observed in the AH (asterisk). In the mutant embryo (R), the OTX2-negative neuroepithelium is lost and the PH and VT domains are merged (arrow in R). (**S,T**) Immunolabelling revealing a lack of ISL1+ve cells in the mutant compared with the control AH (arrows). Note the presence of ISL1+ve cells in both the mutant and control RP (arrowheads). (**U,V**) Double immunofluorescence against N- and E-cadherin (green and red, respectively) showing comparable N-cadherin expression in the hypothalamus between both genotypes (arrows). Note that N-cadherin is not expressed in the anterior region of the mutant RP, which expresses E-cadherin instead, possibly suggesting a posterior expansion of its expression domain in the oral ectoderm (arrowhead in V). (**W,X**) SOX2 expression in the hypothalamus and RP epithelium is comparable between the control and mutant embryo. Abbreviations as in Fig. 1. Scale bar is 100μm.

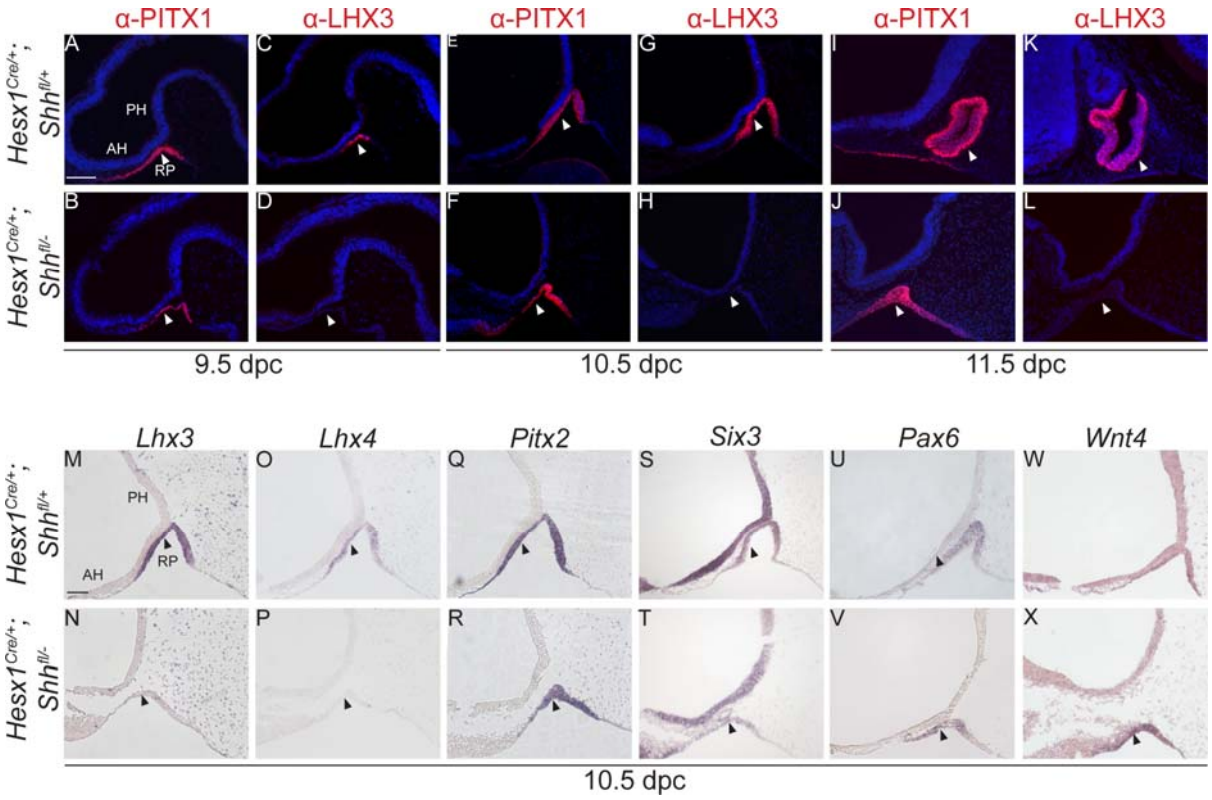

Fig. 6. RP epithelium fails to activate LHX3 and LHX4 expression in *Hesx1*$^{Cre/+}$*;Shh*$^{fl/-}$ mutants. Immunofluorescence and *in situ* hybridisation on mid-sagittal sections on *Hesx1*$^{Cre/+}$*;Shh*$^{fl/-}$ and control embryos against RP progenitor markers. Markers and stages are indicated. **(A-L)** Single immunofluorescent staining showing that while PITX1 expression is maintained, LHX3 is undetectable in the RP of the mutants compared to control embryos from 9.5-11.5dpc (arrowheads). (**M-P**) *In situ* hybridization confirms the lack of *Lhx3* and *Lhx4* expression in the mutant RP at 10.5 dpc (arrowheads). (**Q-X**) Transcripts for other RP markers such as *Pitx2*, *Six3*, *Pax6* and *Wnt4* are detected in the developing mutant and control RP (arrowheads). Abbreviations as in Fig. 1. Scale bar is 100μm.

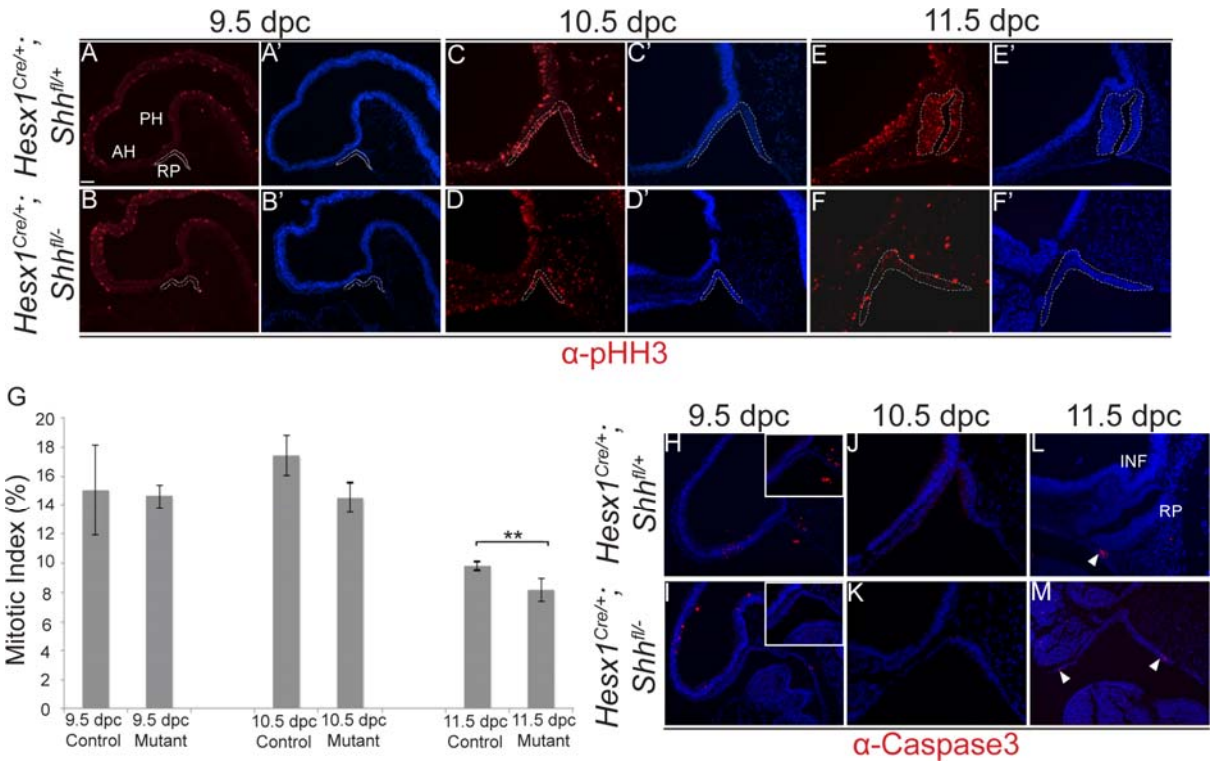

Fig. 7. Reduced proliferation of RP epithelium in *Hesx1*$^{Cre/+}$;*Shh*$^{fl/-}$ mutant embryos. (A-G) Immunofluorescent staining against phospho-Histone H3 (pHH3) on mid-sagittal sections of control and *Hesx1*$^{Cre/+}$;*Shh*$^{fl/-}$ embryos from 9.5 to 11.5 dpc. Note a significant decrease in the mitotic index in the RP epithelium *Hesx1*$^{Cre/+}$;*Shh*$^{fl/-}$ mutant compared with control embryos at 11.5dpc. The mitotic index is the ratio of pHH3+ve cells out of the total DAPI+ve nuclei. Students T-Test: 9.5 dpc, p=0.92; 10.5 dpc, p=0.0645; 11.5 dpc, p<0.001 (n=6 embryos per group). (**H-M**) Immunofluorescence against activated cleaved-Caspase 3 revealing the absence of positive cells in RP epithelium in both genotypes from 9.5 and 10.5 dpc. Apoptotic cells are observed only in the "feet" of the evaginating RP at 11.5 dpc (arrowheads). Mesenchymal cells around RP show reduced staining in the mutant embryo. Positive signal in the cavities is artefactual. Dashed lines delineate the area that was quantified. Abbreviations as in Fig. 1. Scale bars are 100μm.

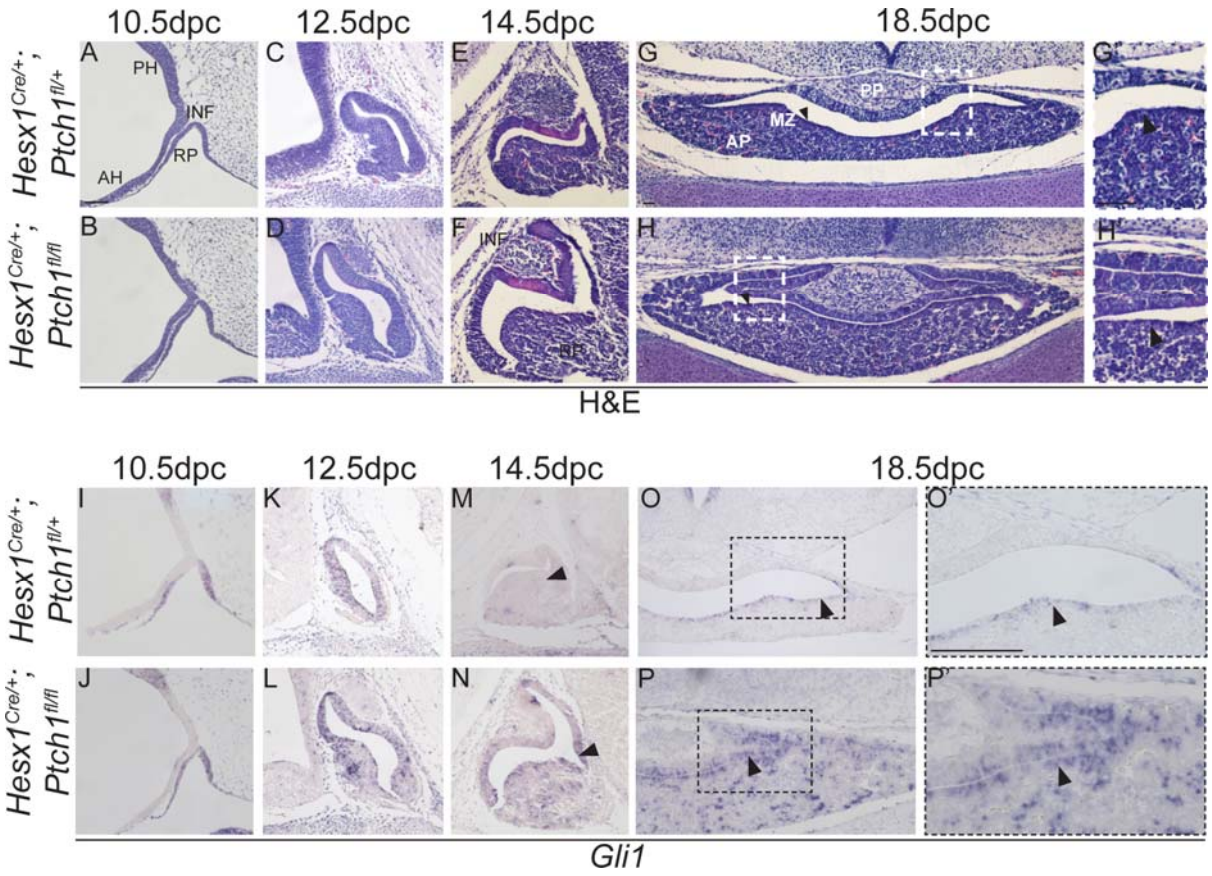

Fig. 8. Conditional deletion of *Ptch1* in *Hesx1*$^{Cre/+}$;*Ptch1*$^{fl/fl}$ mutants results in pituitary hyperplasia. (A-H) Haematoxylin and eosin (H&E) staining on mid-sagittal (A-F) and coronal (G,H) sections of control and *Hesx1*$^{Cre/+}$;*Ptch1*$^{fl/fl}$ embryos throughout pituitary organogenesis. At 10.5 dpc (A,B), the morphology of the RP is comparable between genotypes, but looks slightly expanded in the mutant compared with the control embryo at 12.5 dpc (C,D). By 14.5 dpc (E,F), the *Hesx1*$^{Cre/+}$;*Ptch1*$^{fl/fl}$ anterior pituitary (AP) is clearly hyperplastic relative to the control, but the infundibulum looks normal (INF). AP hyperplasia is also evident at 18.5 dpc (G,H) with dorsal extensions of the cleft. The posterior pituitary (PP) looks comparable between genotypes. Note the expansion of the marginal zone (MZ; arrowheads in G,H), which is thicker in the mutant compared with the control pituitary. G' and H' are insets of the boxed area in G and H. (**I-P**) *In situ* hybridisation against *Gli1*. A remarkable increase in *Gli1* expression is observed throughout the AP in the mutants relative to the control embryos, including the MZ (arrowheads in O and P). O' and P' are insets of the boxed area in O and P. Abbreviations as in Fig. 1. Scale bar is 100μm.

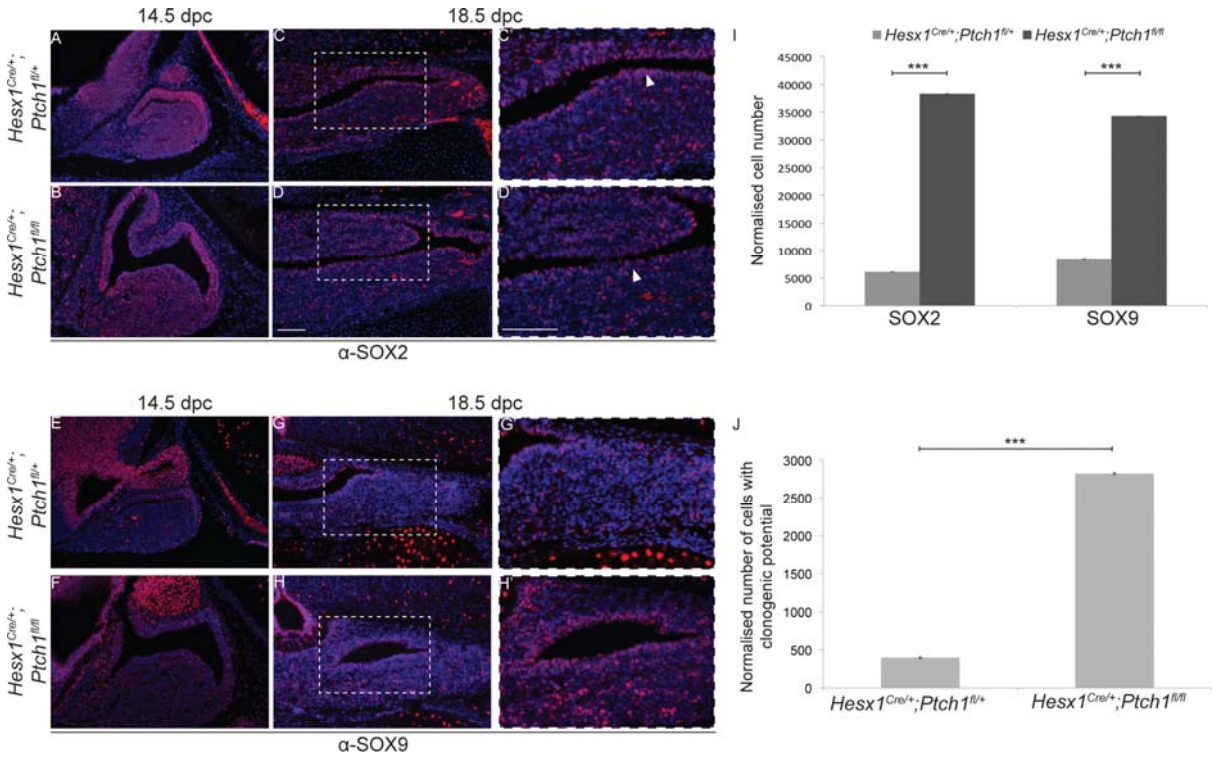

Fig. 9. Increased numbers of SOX2+ve and SOX9+ cells and enhanced clonogenic potential in *Hesx1$^{Cre/+}$;Ptch1$^{fl/fl}$* mutant pituitaries. Immunofluorescence against SOX2 and SOX9 on mid-sagittal (A,B,E,F) and frontal (C,D,G,H) sections of control and *Hesx1$^{Cre/+}$;Ptch1$^{fl/fl}$* mutant embryos at 14.5 and 18.5 dpc. (**A-D**) SOX2 expression is comparable between genotypes at 14.5 dpc, but is clearly expanded in the *Hesx1$^{Cre/+}$;Ptch1$^{fl/fl}$* pituitary relative to the control at 18.5 dpc. Note the thicker marginal zone in the mutant (arrowheads in C' and D') (arrowheads). (C',D') Higher magnification of the boxed region shown in C and D. (**E-H**) An expansion in SOX9 expression is observed in the mutant relative to the control pituitary at both 14.5 and 18.5 dpc. (G',H') Higher magnification of the boxed region shown in G and H. (**I,J**) Quantitative analysis confirms the expansion of the SOX2+ve and SOX9+ve cell compartment at 18.5 dpc. (**K**) Quantification of the clonogenic potential of the pituitary in *Hesx1$^{Cre/+}$;Ptch1$^{fl/fl}$* mutants and control embryos at 18.5 dpc. A significant 3.4 fold increase is observed in the mutant pituitaries (n=6, $p<0.01$; bars represent means ± SD, Student's T-test). Scale bars are 100μm.

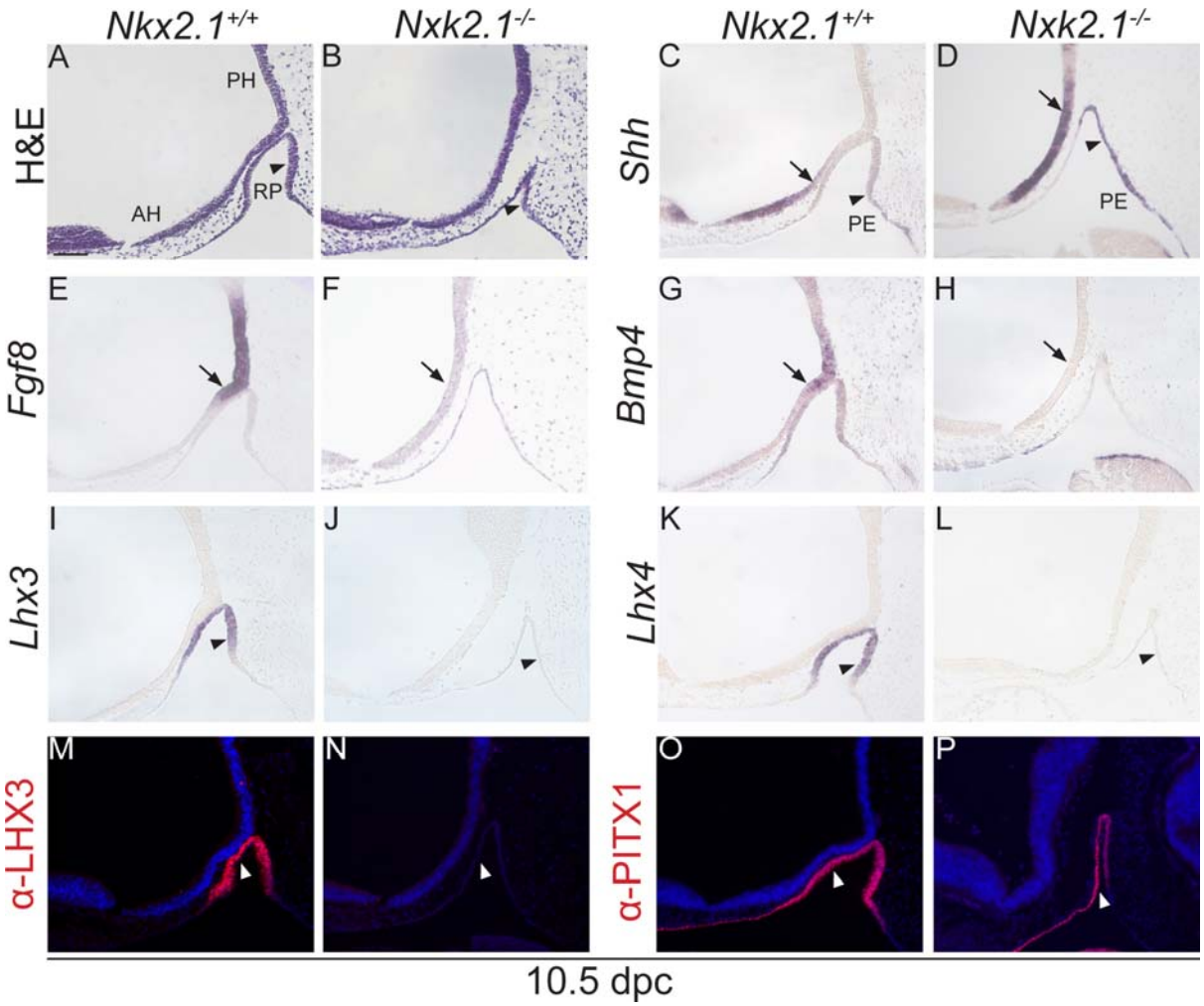

Fig. 10. Failure to activate *Lhx3* and *Lhx4* expression in the developing RP of *Nk2.1*$^{-/-}$ mutants. Haematoxylin and eosin (H&E) and RNA *in situ* hybridisation on mid-sagittal sections of *Nkx2.1*$^{-/-}$ mutants and *Nkx2.1*$^{+/+}$ control embryos at 10.5 dpc. (**A,B**) Note that Rathke's pouch (RP) is hypoplastic in the *Nkx2.1*$^{-/-}$ mutant compared with the *Nkx2.1*$^{+/+}$ control (arrowheads) and does not contact the overlying hypothalamus. (**C-D**) *Shh* transcripts are detected in the hypothalamus, but the expression domain is posteriorised in the mutant relative to the control embryo (arrows). Note the ectopic expression of *Shh* in the posterior region of RP in the mutant compared with the control embryo (arrowheads), suggesting an anteriorisation of the *Shh* expression domain in the pharyngeal endoderm (PE). (**E-H**) *Fgf8* and *Bmp4* expression domains in the posterior hypothalamus are completely lost in the mutant embryos (arrows). (**I-L**) *In situ* hybridisation revealing the total absence of both *Lhx3* and *Lhx4* expression in the RP of the mutants (arrowheads). (**M-P**) Immunostaining

confirms the lack of LHX3 expression and reveals the expression of PITX1 in the mutant pituitary (arrowheads). Abbreviations as in Fig. 1. Scale bar: 100μm.

Tables

Table 1 - Genotypes obtained from *Hesx1*$^{Cre/+}$;*Shh*$^{+/-}$ x *Shh*$^{fl/fl}$ intercrosses.

Stage	Genotypes (% expected)[a]				
	Hesx1$^{+/+}$; *Shh*$^{fl/+}$ (25%)	*Hesx1*$^{+/+}$; *Shh*$^{fl/-}$ (25%)	*Hesx1*$^{Cre/+}$; *Shh*$^{fl/+}$ (25%)	*Hesx1*$^{Cre/+}$; *Shh*$^{fl/-}$ (25%)	**Total**
9.5 dpc	10	12	14	12	48
10.5 dpc	27	23	26	28	104
11.5 dpc	9	8	9	7	33
12.5 dpc	11	14	12	10	47
14.5 dpc	8	10	15	14	47
16.5 dpc	14	12	12	13	51
18.5 dpc	8	9	11	3	31
Embryos[b] (%observed)	87 (24.1%)	88 (24.3%)	99 (27.4%)	87 (24.1%)	361
Pups (%observed)	19 (28.4%)	24 (35.8%)	26 (38.8%)	0[*]	67

[a] Derived from expected Mendelian ratios.

[*] Chi-square test revealed a significant deviation from the expected 25% ratio (P<0.001).

[b] Chi-square test revealed no significant deviation from the expected Mendelian ratios.

Table 2 - Genotypes obtained from *Hesx1*$^{Cre/+}$;*Ptch1*$^{fl/+}$ x *Ptch1*$^{fl/fl}$ intercrosses.

Stage	Genotypes (% expected)[a]				Total
	Hesx1$^{+/+}$; *Ptch1*$^{fl/+}$ (25%)	*Hesx1*$^{+/+}$; *Ptch1*$^{fl/fl}$ (25%)	*Hesx1*$^{Cre/+}$; *Ptch1*$^{fl/+}$ (25%)	*Hesx1*$^{Cre/+}$; *Ptch1*$^{fl/fl}$ (25%)	
10.5 dpc	7	8	7	9	31
11.5 dpc	5	7	6	6	24
12.5 dpc	9	6	8	10	36
14.5 dpc	9	8	7	7	28
16.5 dpc	7	4	9	8	28
18.5 dpc	12	14	16	15	57
Embryos[b] (%observed)	49 (24%)	47 (23%)	53 (26%)	55 (27%)	204
Pups (%observed)	26 (39%)	21 (32%)	19 (29%)	0[*]	66

[a] Derived from expected Mendelian ratios.

[*] Chi-square test revealed a significant deviation from the expected 25% ratios (P<0.001).

[b] Chi-square test revealed no significant deviation from the expected Mendelian ratios.

SUPPLEMENTARY TEXT

Supplementary Materials and Methods

Mice and human pituitaries

Mice and embryos were genotyped using an ear or tail biopsy, respectively. DNA was extracted using a 20ul solution of a 1 in 5 dilution of DNAreleasy (Anachem) according to the manufacturer's instructions. The data presented in this work is representative from at least 3 individual embryos per genotype. All animal procedures were carried out under the Animals (Scientific Procedures) fully compliant with the current Home Office legislation.

Histology and *in situ* hybridisation on histological sections

The antisense riboprobes used in this study (*Shh*, *Bmp4*, *Fgf8*, *Lhx3*, *Lhx4*, *Pax6*, *Six3*, *Wnt5a*, *Tbx2*, *Tbx3*, *Nxk2.1*, *Pomc1*, *Ghrh*, *Gnrh*, *Ss*, *Ot* and *Gnrh*) have been described previously (Gaston-Massuet et al., 2011; Jayakody et al., 2012; Trowe et al., 2013). Full-length human antisense riboprobe against *GLI1* was obtained from Source Bioscience (BE296931).

Immunofluorescence

Detection of hormones were carried out using antibodies for GH (NHPP AFP-5641801), ACTH (10C-CR1096M1), TSH (NHPP AFP-1274789), PRL (NHPP AFP-425-10-91), LH (NHPP AFP-C697071P) and FSH (AFP-7798-1289) (Developmental Studies Hybridoma Bank) at a 1:1000 dilution. Detection of pituitary lineage commitment markers was performed using antibodies for PIT1 (Gift from S. Rhodes), TPIT (Gift from J. Drouin) and GSU (Developmental Studies Hybridoma Bank) at a 1:1000 dilution. of 1:200. Markers of pituitary stem cells-SOX2 (GT15098, Immune Systems) and SOX9 (AB5535, Milipore) were used at a dilution of 1:250 and 1:500, respectively. Cruz). Detection of activated BMP4 and FGF responding cells was performed using pERK1/2 (9101, Cell Signaling) and pSMAD1/5/8 (41D10, Cell Signaling) at a dilution of 1:250. Proliferation marker pHH3 was

used at a 1:155 dilution (06-570, Millipore). Pituitary markers PITX1 (Gift from J. Drouin), LHX3 (67.4E12, Developmental Studies Hybridoma Bank) and ISL1 (K-20, Santa Cruz) were used at a dilution of 1:1000. Anterior hypothalamic markers SHH (AF464, R&D Systems), TCF4 (05-511, Millipore) and OTX2 (sc-514195, Santa Cruz) were used at a dilution of 1:100. N-cadherin (ab18203, Abcam) and E-cadherin (610181, BD BioScience) were used at a 1:100 dilution. Histological sections were counterstained with DAPI (Sigma).

RNA sequencing of dissected Rathke's pouch epithelium

Rathke's pouch was dissected from wild-type embryos at 10.5 dpc. RNA was extracted using RNeasy Micro Kit (Qiagen). RNA quality and concentration was measured using the 2100 Bioanalyzer. Extracted RNA was then sent to Wellcome Trust Genomics unit, Oxford University for RNA sequencing. Library preps made using the Smarter kit (High Vol #634828) from Clonetech/Takara and PolyA-Illumina's TruSq stranded kit (RS-122-2103 #E6040L) from New England Bioloabs. RNA sequencing was performed using the SMARTer-seq low input RNA kit. RNA sequencing parameters were 80bp, double ends and 15 million read depth with amplification. Alignment against mm10 reference genome was performed using Stampede. Per gene read counts were calculated using RSubread, differential analyses was performed using DESEq2 and ontology analysis using GOSeq (Liao et al., 2013; Love et al., 2014; Young et al., 2010). For gene set enrichment analysis (GSEA), genes were ranked by their Wald statistic and GSEA performed using the pre-ranked tool in GSEA v2.2.3 (Broad Institute) (Subramanian et al., 2005). The Hallmark Sonic Hedgehog pathway geneset was downloaded from the Molecular Signature Database v5.2 (Broad Institute) (Subramanian et al., 2005).

Assessment of clonogenic potential

Pituitaries were dissected using aseptic forceps and the posterior pituitary was removed. The anterior lobe was minced with forceps and placed into 200ul of Enzyme mix, which consists of Hanks' Balanced Salt Solution (HBSS, Gibco), 0.5% w/v Collagenase (Worthington),

50ug/ml (Worthington), 1% Fungizone and 0.1X trypsin (Sigma), for 4 hours in a 37ºC water bath. HBSS was added to make a final volume of 500ul post incubation and the solution was triturated into a single cell suspension. Once single cell suspension was achieved, 9.5ml of HBSS is added and the cells are spun down for 5 minutes at 1000rpm. Cells were re-suspended in growth medium, which consists of DMEM/F12, 5% FCS, 1% PenStrep, 20ng/ml human recombinant bFGF (R&D Systems) and 50ng/ml cholera toxin. Cells were plated at clonal density in a 6-well plate at 2000, 4000 and 8000 cells per well. Media was changed every 3 days after colony establishment. To count the number of colonies, after 7 days, colonies were washed with 1X PBS and fixed for 20 minutes with 4% PFA. Colonies were stained with Harris' haematoxylin for 15 minutes at RT. The proportion of colonies observed relative to seeded cells was used to estimate total clonogenic cells in 18.5 dpc pituitaries by multiplying this value with the total number of cells in the dissociated pituitary.

Table S1. Pituitary Gene Ontology

Category	over_repr	numDEIn	numInCat	term	ontology	padj
GO:00219	0.000167	4	38	Pituitary	BP	0.046803

Table S2. Genes involved in pituitary development.

*Fold Change	Gene Symbol	Adjusted p-value
4.231324889	*Pitx1*	0.006657901
5.105959333	*Prop1*	0.000884996
1.575755361	*Bmp2*	0.999855699
27.69985383	*Lhx4*	5.74E-21
16.90654044	*Lhx3*	3.31E-14
44.21160974	*Hesx1*	2.99E-30
0.639540028	*Pax6*	0.999855699
1.031192461	*Sox2*	0.999855699
0.091398855	*Pax3*	2.73E-09
0.892479935	*Tcf3*	0.999855699
1.96329081	*Six3*	0.488932014
1.459287982	*Isl1*	0.999855699

* higher than 1.0 means up-regulated in the wild-type RP

Supplementary References

Gaston-Massuet, C., Andoniadou, C. L. C. L., Signore, M., Jayakody, S. a, Charolidi, N., Kyeyune, R., Vernay, B., Jacques, T. S., Taketo, M. M., Le Tissier, P., et al. (2011). Increased Wingless (Wnt) signaling in pituitary progenitor/stem cells gives rise to pituitary tumors in mice and humans. *Proc. Natl. Acad. Sci. U. S. A.* **108**, 11482–11487.

Jayakody, S. A., Andoniadou, C. L., Gaston-massuet, C., Signore, M., Cariboni, A., Bouloux, P. M., Tissier, P. Le, Pevny, L. H., Dattani, M. T. and Martinez-barbera, J. P. (2012). SOX2 regulates the hypothalamic-pituitary axis at multiple levels. *J. Clin. Invest.* **122**, 3635–3646.

Liao, Y., Smyth, G. K. and Shi, W. (2013). The Subread aligner: fast, accurate and scalable read mapping by seed-and-vote. *Nucleic Acids Res.* **41**, e108.

Love, M. I., Huber, W. and Anders, S. (2014). Moderated estimation of fold change and dispersion for RNA-seq data with DESeq2. *Genome Biol.* **15**, 550.

Subramanian, A., Tamayo, P., Mootha, V. K., Mukherjee, S., Ebert, B. L., Gillette, M. A., Paulovich, A., Pomeroy, S. L., Golub, T. R., Lander, E. S., et al. (2005). Gene set enrichment analysis: A knowledge-based approach for interpreting genome-wide expression profiles. *Proc. Natl. Acad. Sci.* **102**, 15545–15550.

Trowe, M.-O., Zhao, L., Weiss, A.-C., Christoffels, V., Epstein, D. J. and Kispert, A. (2013). Inhibition of Sox2-dependent activation of Shh in the ventral diencephalon by Tbx3 is required for formation of the neurohypophysis. *Development* **140**, 2299–2309.

Young, M. D., Wakefield, M. J., Smyth, G. K., Oshlack, A., Fu, X., Fu, N., Guo, S., Yan, Z., Xu, Y., Hu, H., et al. (2010). Gene ontology analysis for RNA-seq: accounting for selection bias. *Genome Biol.* **11**, R14.

Supplementary Figures

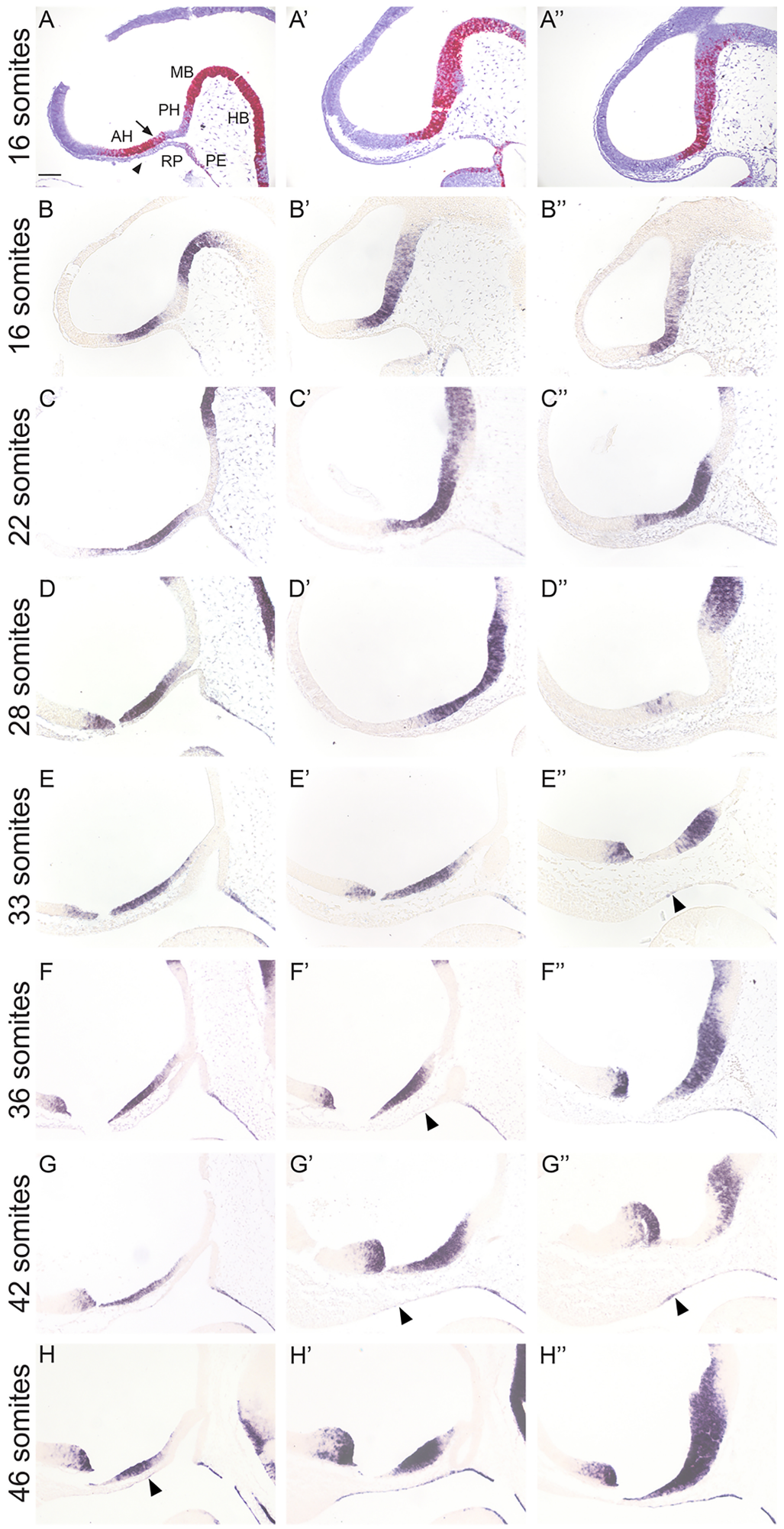

Figure S1. *Shh* is expressed in the oral ectoderm in wild-type embryos by the 33 somite stage. RNA *in situ* hybridisation on sagittal histological sections of wild-type embryos between 16 and 46 somites. Three different levels are shown from approximately midline sagittal (A-H), medio-lateral (A′-H′) and lateral (A′′-H′′). (**A-D**) From 16 to 28 somites *Shh* transcripts are detected in the midline anterior hypothalamus (AH, arrow), posterior hypothalamus (PH) and pharyngeal endoderm (PE) abutting the developing Rathke's pouch (RP). No expression is observed in the developing oral ectoderm at these stages (arrowhead). (**E**) At 33 somites, *Shh* transcripts are weakly detected in the lateral oral ectoderm (arrowhead) and pharyngeal endoderm. (**F-H**) Stronger *Shh* expression is observed in the medio-lateral and lateral oral ectoderm from the 36 somite-stage (arrowheads). Abbreviations: RP, Rathke's pouch; PH, posterior hypothalamus; AH, anterior hypothalamus; PE, pharyngeal endoderm; MB, midbrain; HB, hindbrain. Scale bar is 100μm.

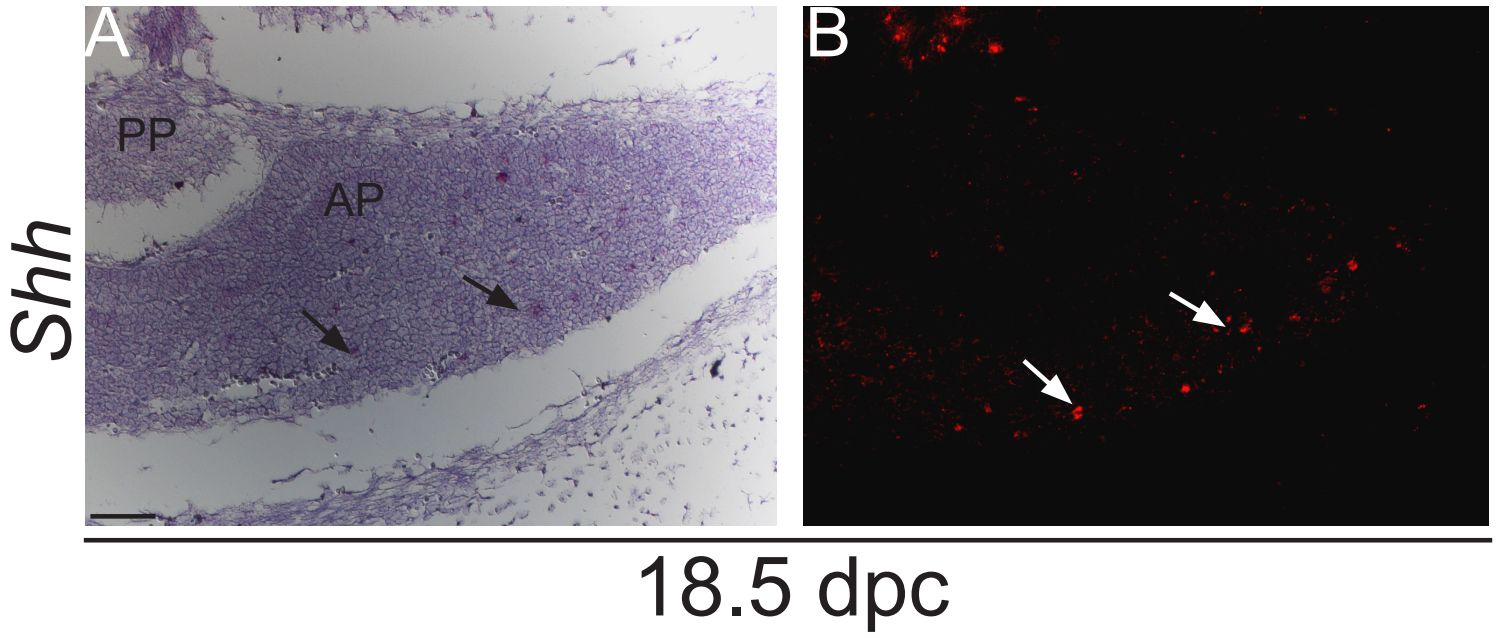

Figure S2. *Shh* mRNA is detectable in single cells within the anterior pituitary at 18.5 dpc. (A,B) RNA *in situ* hybridisation using the RNAscope (ACDBio) procedure on frontal sections of wild-type embryos at the level of the pituitary gland. Note the presence of positive foci within the anterior pituitary in both the bright field (A) and fluorescent picture (B) (arrows).

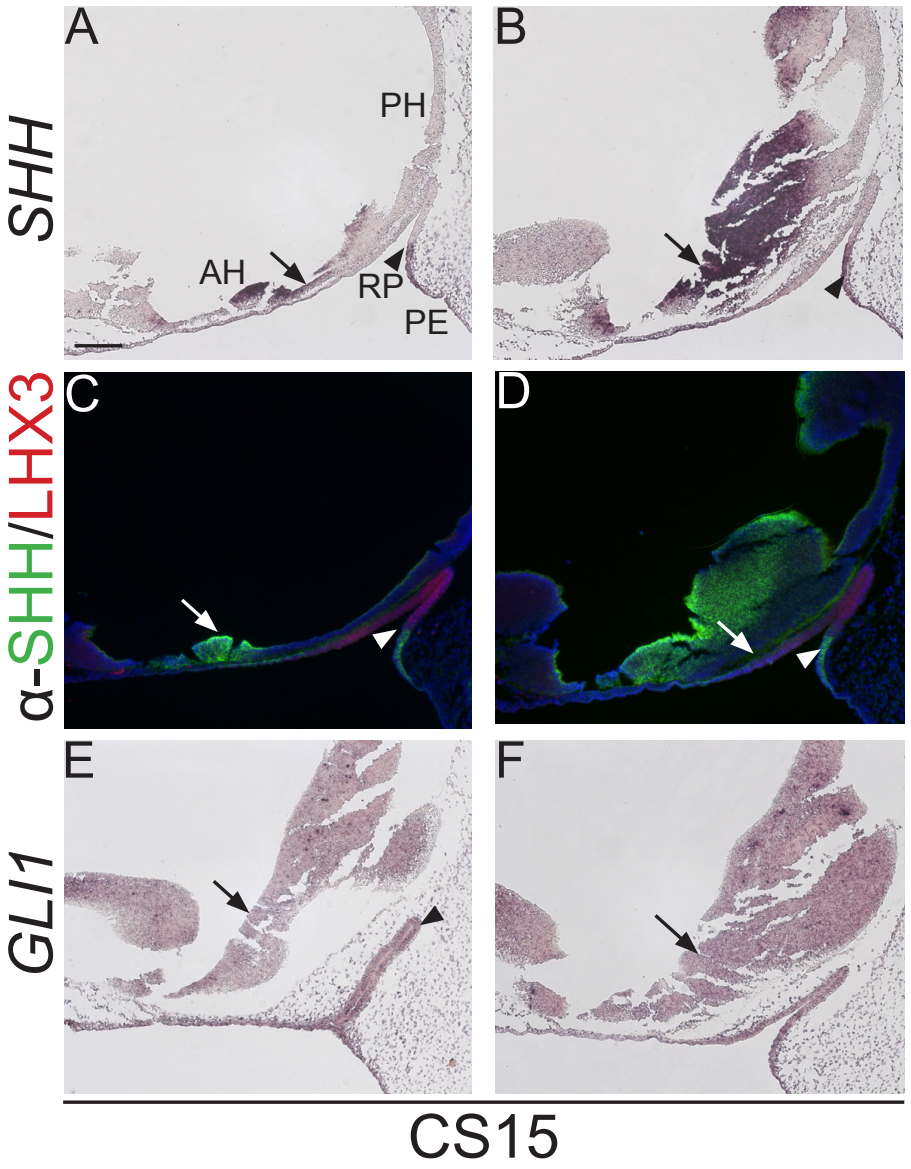

Figure S3. *SHH* and *GLI1* are expressed in human fetal pituitaries. *In situ* hybridisation and double immunofluorescence on two non-consecutive mid sagittal sections of human fetal pituitaries at Carnegie stage 15 (CS15). (**A,B**) *SHH* transcripts are expressed in the anterior hypothalamus (AH, arrows) and pharyngeal endoderm (PE), but not in the developing Rathke's pouch (RP) (arrowheads). (**C,D**) SHH immunostaining (green signal) confirms the expression in the AH (arrow) and PE, but not in RP, which is positive for LHX3 (red signal). (**E,F**) *GLI1* transcripts are found throughout the hypothalamus (arrows) and RP (arrowheads). Abbreviations: AH, anterior hypothalamus; RP, Rathke's pouch; PE, pharyngeal endoderm; PH, posterior hypothalamus. Scale bar: 100µm.

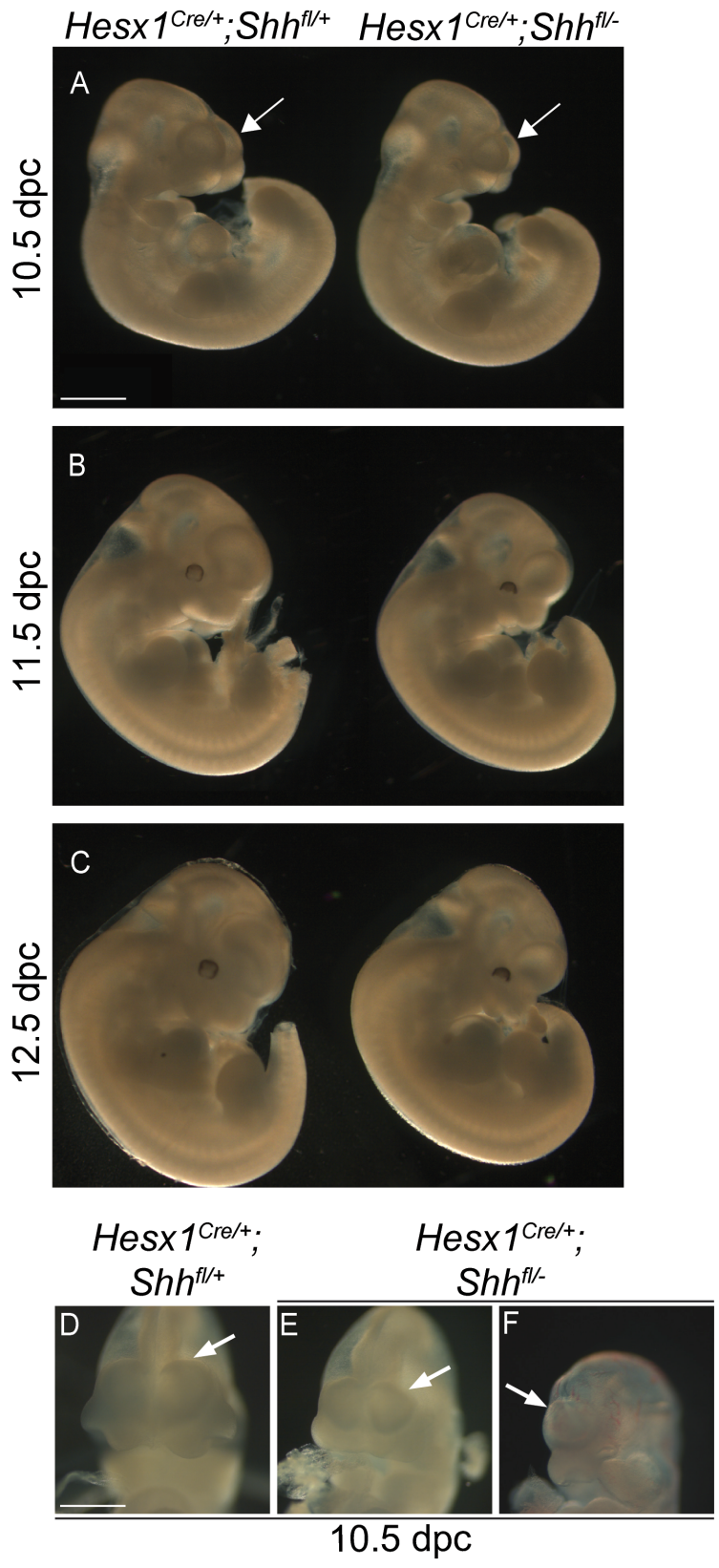

Figure S4. Forebrain defects in *Hesx1$^{Cre/+}$;Shh$^{fl/-}$* embryos. (**A-F**) *Hesx1$^{Cre/+}$;Shh$^{fl/+}$ and Hesx1$^{Cre/+}$;Shh$^{fl/-}$* embryos from 10.5 to 12.5 dpc showing small telencephalic vesicles (arrows) and eye defects. (**G-I**) Frontal view a control embryo and two *Hesx1$^{Cre/+}$;Shh$^{fl/-}$* mutants at 10.5 dpc, showing the small telencephalic vesicles (H) and holoprosencephaly (I). Scale bar: 1mm.

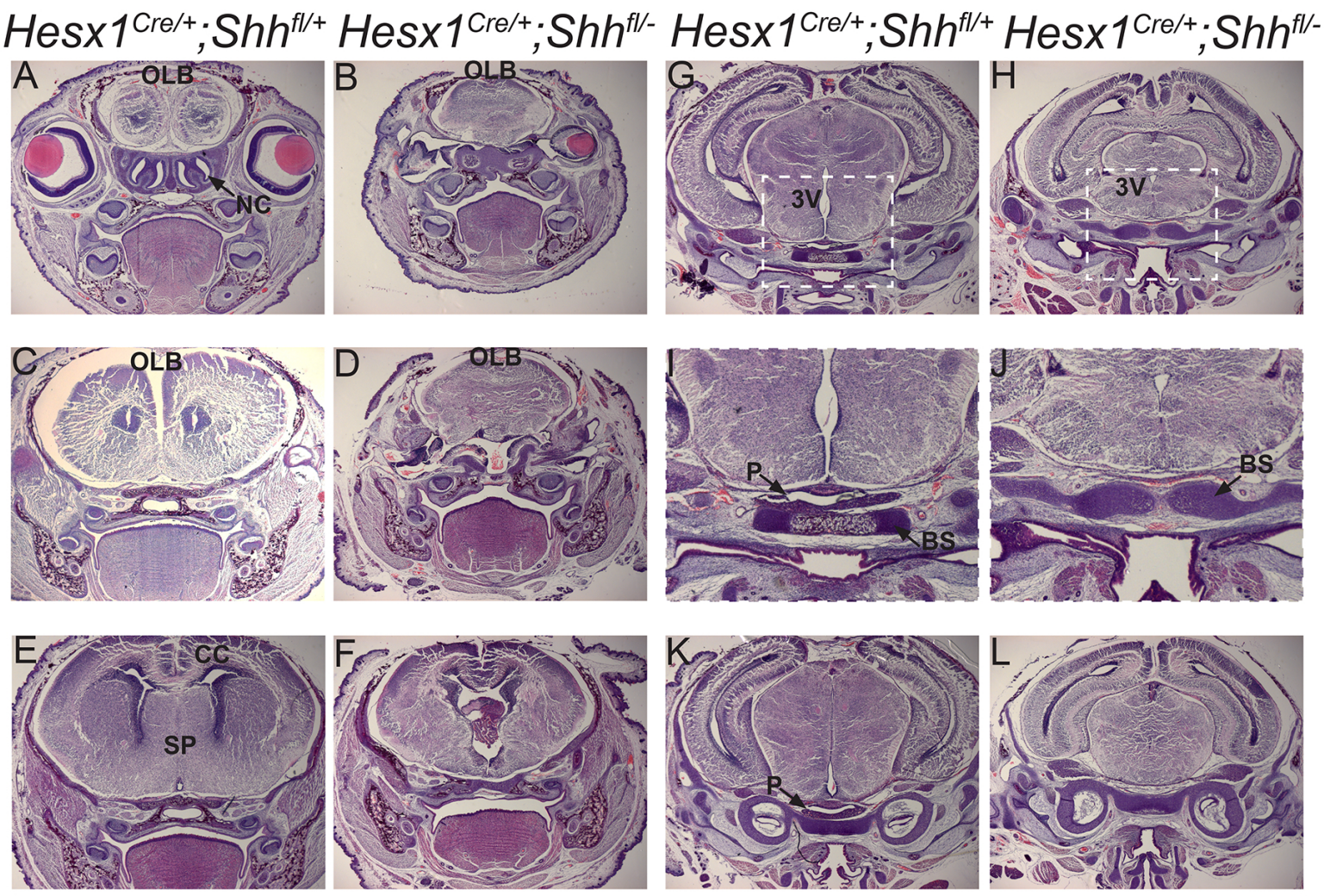

Figure S5. Craniofacial defects and loss of pituitary tissue in *Hesx1*$^{Cre/+}$;*Shh*$^{fl/-}$ mutants at 18.5 dpc. Haematoxylin and eosin (H&E) staining on frontal sections from the eyes to the posterior hypothalamus in *Hesx1*$^{Cre/+}$;*Shh*$^{fl/-}$ mutant and control embryos at 18.5 dpc. (**A-F**) *Hesx1*$^{Cre/+}$;*Shh*$^{fl/-}$ mutants show eye defects (microphthalmia or anophthalmia), fused olfactory bulbs (OLB), deformed nasal cavity (NC) and absent of the septum pellucidum (SP) and corpus callossum (CC). (**G-J**) At more posterior levels, the two cerebral hemispheres are identifiable, but the entire brain is smaller in the mutant relative to the control embryo, and the pituitary (P, arrows in I and K) is absent in the mutant. Abbreviations: 3V, third ventricle; BS, basisphenoid bone; NC, nasal cavity; OLB olfactory bulbs; P, pituitary. Scale bar: 100 μm.

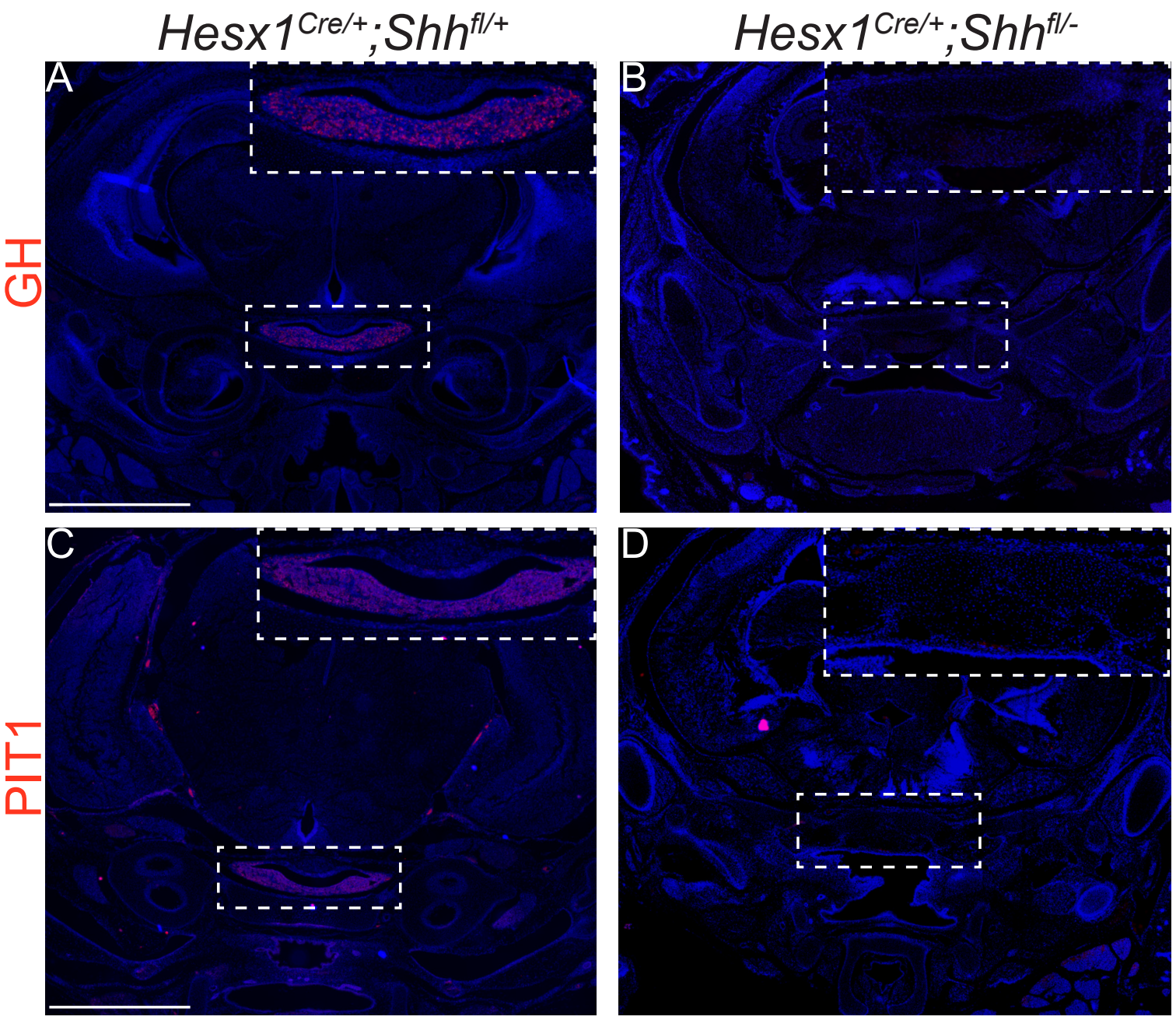

Figure S6. Loss GH+ve and PIT1+ve cells in the *Hesx1*$^{Cre/+}$;*Shh*$^{fl/-}$ mutant pituitary at 18.5 dpc. Immunofluorescence against GH (A,B) and PIT1 (C,D) on frontal sections from control and *Hesx1*$^{Cre/+}$;*Shh*$^{fl/-}$ mutant embryos at 18.5 dpc. No positive signal is detectable in the mutant pituitary. Scale bar: 100 μm.

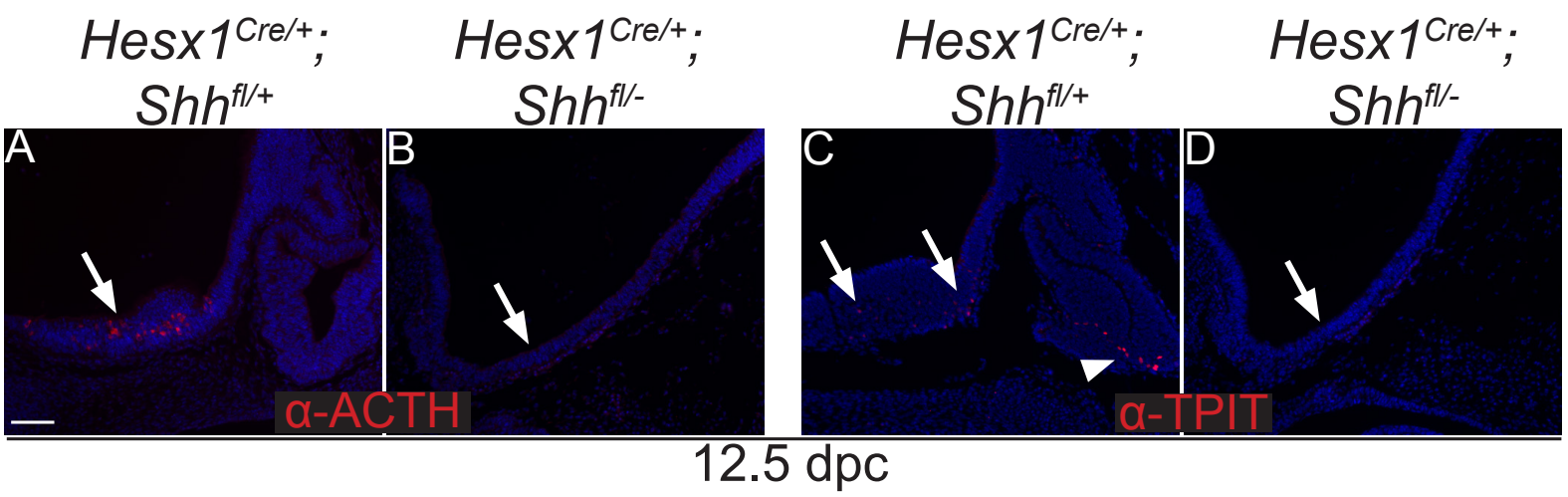

Figure S7. ACTH+ve and TPIT+ve cells are lost in the anterior hypothalamus of *Hesx1$^{Cre/+}$;Shh$^{fl/-}$* mutants. (**A-D**) Immunofluorescence against ACTH (A,B) and TPIT (C,D) on mid-sagittal sections from control and *Hesx1$^{Cre/+}$;Shh$^{fl/-}$* mutant embryos at 12.5 dpc. ACTH+ve and TPIT+ve cells are present in the anterior hypothalamus of control embryos but not *Hesx1$^{Cre/+}$;Shh$^{fl/-}$* mutants (arrows). Note the present of TPIT+ve cells in the control pituitary. Scale bar: 100µm.

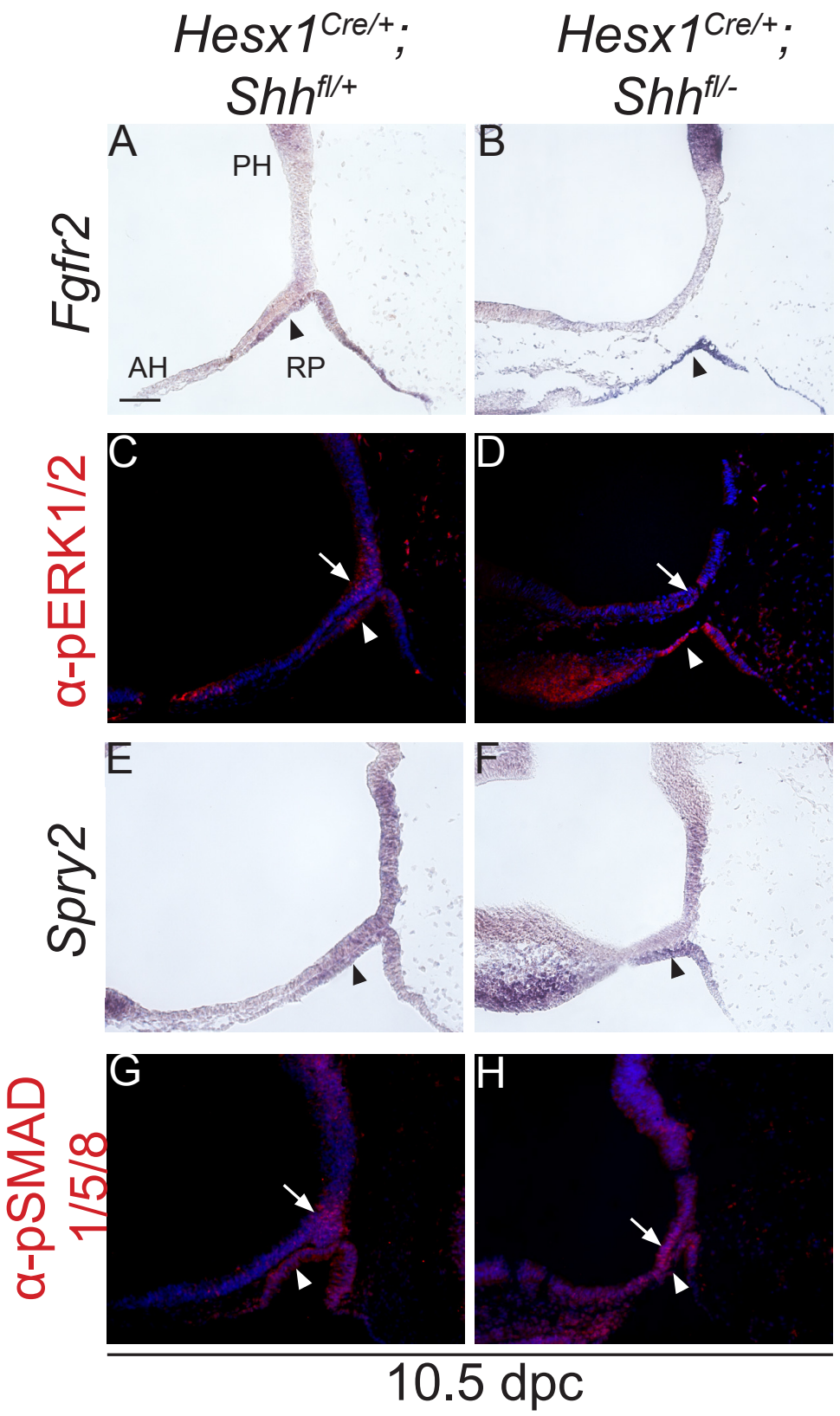

Figure S8. RP is competent to respond to BMP and FGF signalling in *Hesx1*$^{Cre/+}$;*Shh*$^{fl/-}$ mutants. *In situ* hybridisation and immunofluorescence on mid-sagittal sections of *Hesx1*$^{Cre/+}$;*Shh*$^{fl/-}$ mutants and control embryos at 10.5 dpc. (**A,B**) *Fgfr2* transcripts are observed in the control Rathke's pouch (RP) as well as in the rudimentary mutant RP (arrowheads). (**C,D**) Immunofluorescence against p-ERK1/2 reveals positive staining in the hypothalamus and developing RP in both genotypes, suggesting active FGF signalling. (**E,F**) *Spry2*, a direct target of the FGF pathway, is expressed in the hypothalamus and RP in the mutant and control embryo. (**G,H**) Immunofluorescence against p-SMAD1/5/8, a readout of active BMP signalling, showing specific signal in the hypothalamus and RP in both genotypes. Note that head mesenchyme is more abundant in the mutant embryos and expresses pERK1/2, *Spry2* and p-SMAD1/5/8. Scale bar: 100µm.

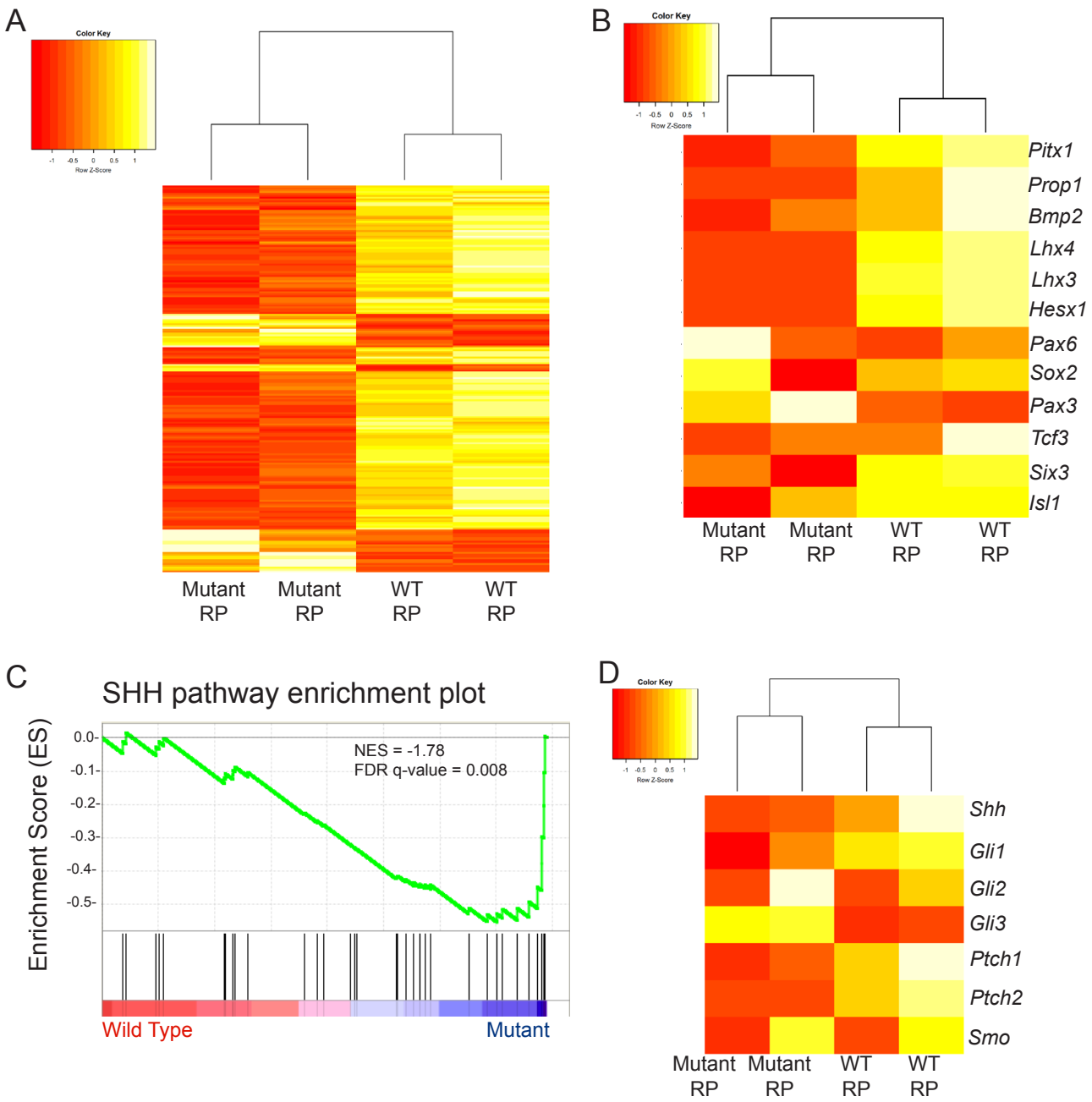

Figure S9. RNA Sequencing data confirms the disruption of RP development in *Hesx1*$^{Cre/+}$;*Shh*$^{fl/-}$ RP at 10.5 dpc. RP from control and mutant embryos (n=2 per group) were manually dissected at 10.5 dpc and subjected to RNA-Sequencing. (**A**) Heatmap representation of the 208 significantly differentially expressed genes between in *Hesx1*$^{Cre/+}$;*Shh*$^{fl/-}$ mutant and control RPs. (**B**) Heatmap representation of 12 functionally important genes during RP and pituitary development, including *Lhx3* and *Lhx4*, revealing the overall down-regulation in their expression levels in the *Hesx1*$^{Cre/+}$;*Shh*$^{fl/-}$ mutant compared with the control RPs. (**C**) Gene set enrichment analysis (GSEA) of differentially expressed genes in mutant RP revealing a negative enrichment for the SHH pathway (Broad Institute) NES: Normalised enrichment score. FDR: False discovery rate. (**D**) Heatmap representation of differentially expressed genes involved in the SHH pathway in *Hesx1*$^{Cre/+}$;*Shh*$^{fl/-}$ mutant and control RP. Note the up-regulation of *Gli1*, *Gli2*, *Ptch1*, *Ptch2* and *Smo* expression levels in the control relative to but the mutant RP. Likewise, *Shh* itself is up-regulated in the control data set. In contrast, *Gli3* expression, a negative regulator of the SHH pathway is up-regulated in the *Hesx1*$^{Cre/+}$;*Shh*$^{fl/-}$ mutant RP.

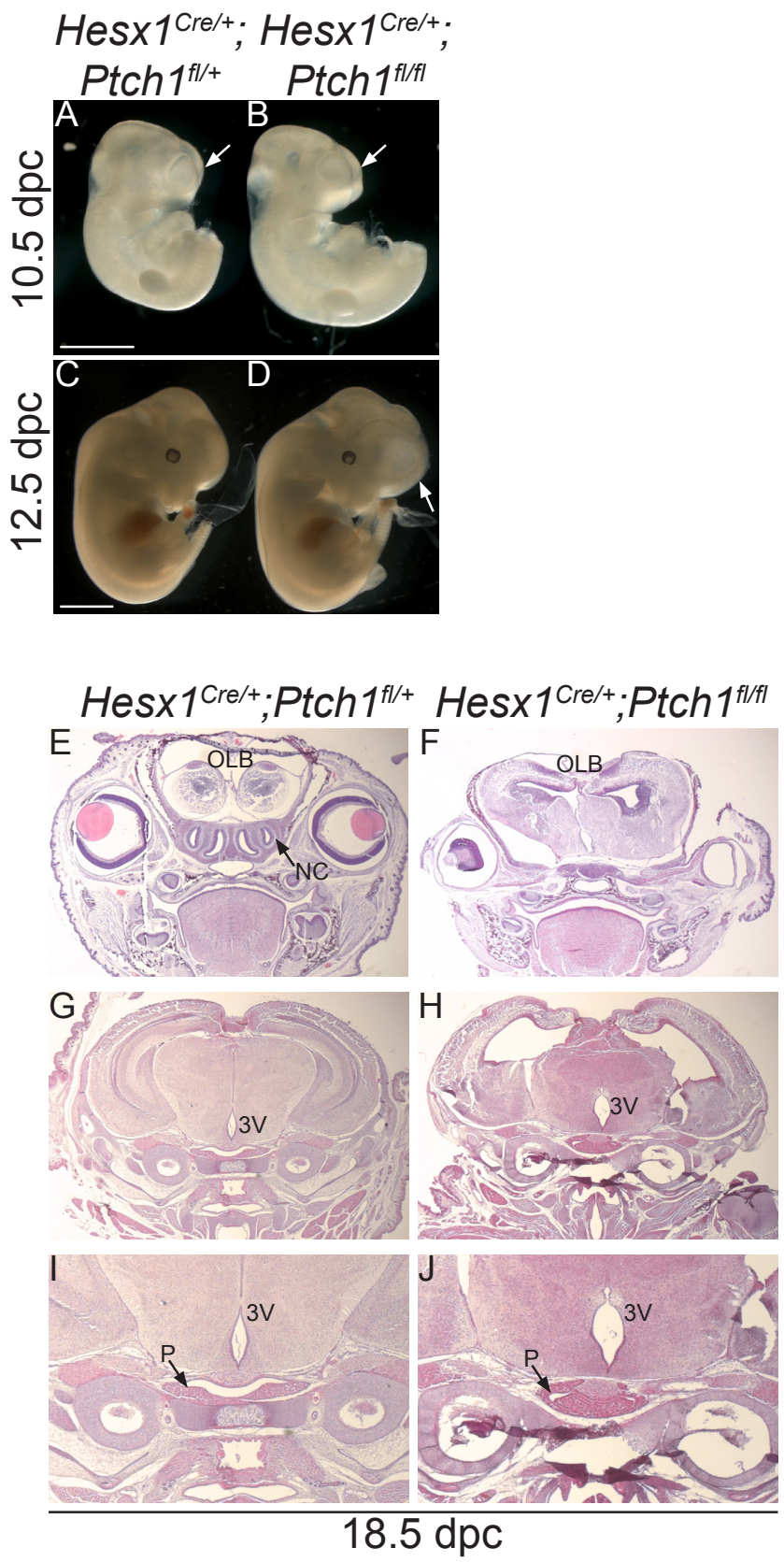

Figure S10. Forebrain and craniofacial defects in the *Hesx1*$^{Cre/+}$;*Ptch1*$^{fl/fl}$ mutants. (**A-D**) *Hesx1*$^{Cre/+}$;*Ptch1*$^{fl/+}$ controls and *Hesx1*$^{Cre/+}$;*Ptch1*$^{fl/fl}$ mutants at 10.5dpc and 12.5 dpc showing the enlargement of the telencephalic vesicles (arrows) . (**E-H**) Haematoxylin and eosin (H&E) staining on frontal sections from the eyes to the posterior hypothalamus in *Hesx1*$^{Cre/+}$;*Ptch1*$^{fl/+}$ controls and *Hesx1*$^{Cre/+}$;*Ptch1*$^{fl/fl}$ mutants at 18.5 dpc. Note the expansion of the olfactory bulbs (OLB), nasal cavity defects (NC) and enlarged pituitary gland (P) in the mutant relative to the control embryo. Scale bar: 100 μm.

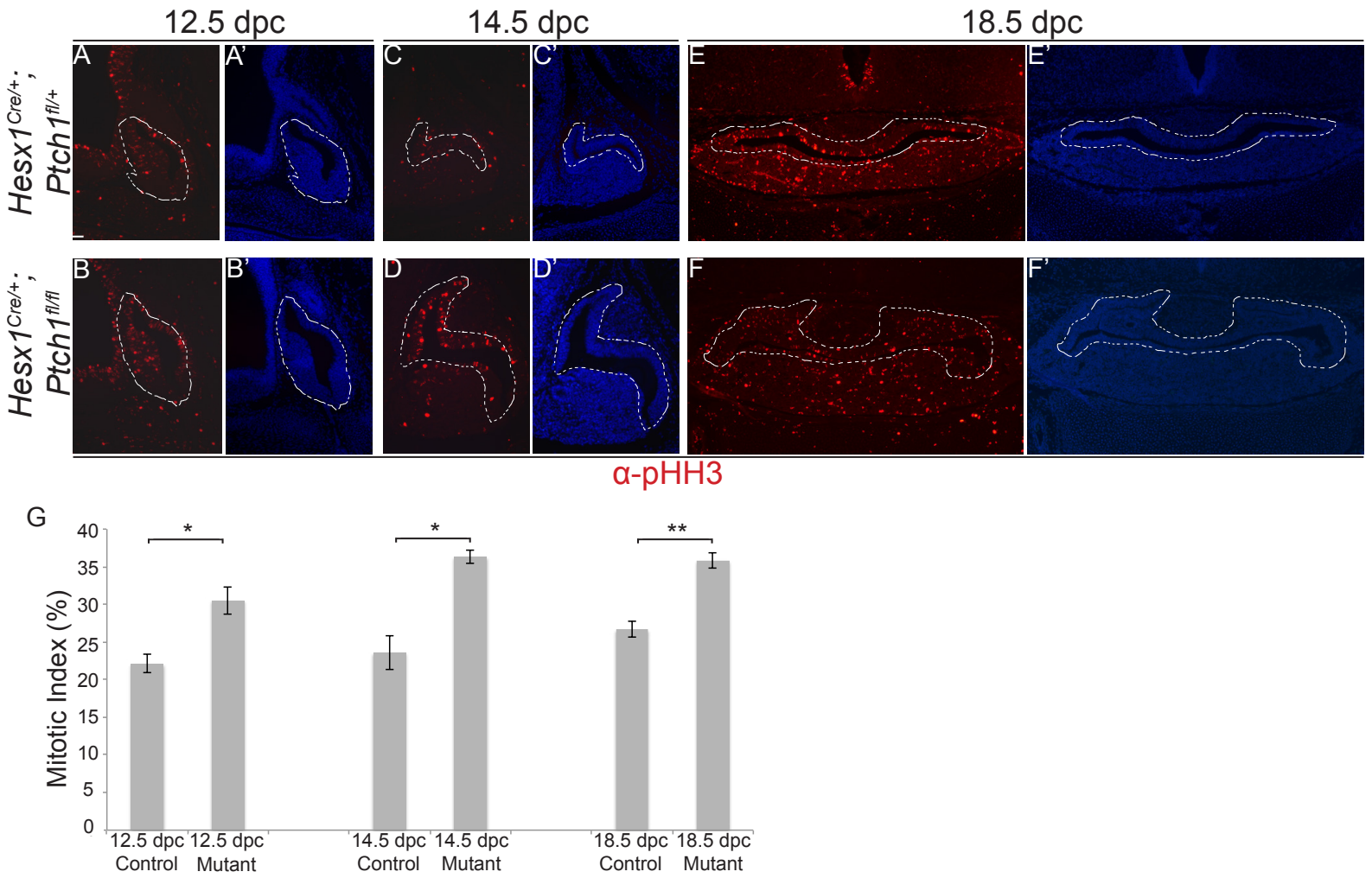

Figure S11. Increased proliferation in *Hesx1*$^{Cre/+}$;*Ptch1*$^{fl/fl}$ pituitaries. (**A-F**) Immunofluorescence against phospho-Histone H3 (pHH3) on mid-sagittal (A-D) and coronal (E,F) sections of control embryos and *Hesx1*$^{Cre/+}$;*Ptch1*$^{fl/fl}$ mutants at 12.5 dpc, when the earliest morphological hyperplasia is visible up, to 18.5 dpc. (**G**) Quantitative analysis revealing the significant increase in the mitotic index in the developing pituitary (i.e. ratio of pHH3+ve cells and DAPI+ve stained nuclei) in the mutants compared with control at all stages analysed. Dashed lines delineate the area that was quantified. Students T-Test: 12.5 dpc, p=0.03; 14.5 dpc, p=0.04; 18.5 dpc, P=0.008; n=6 for each group. Scale bars: 100μm.

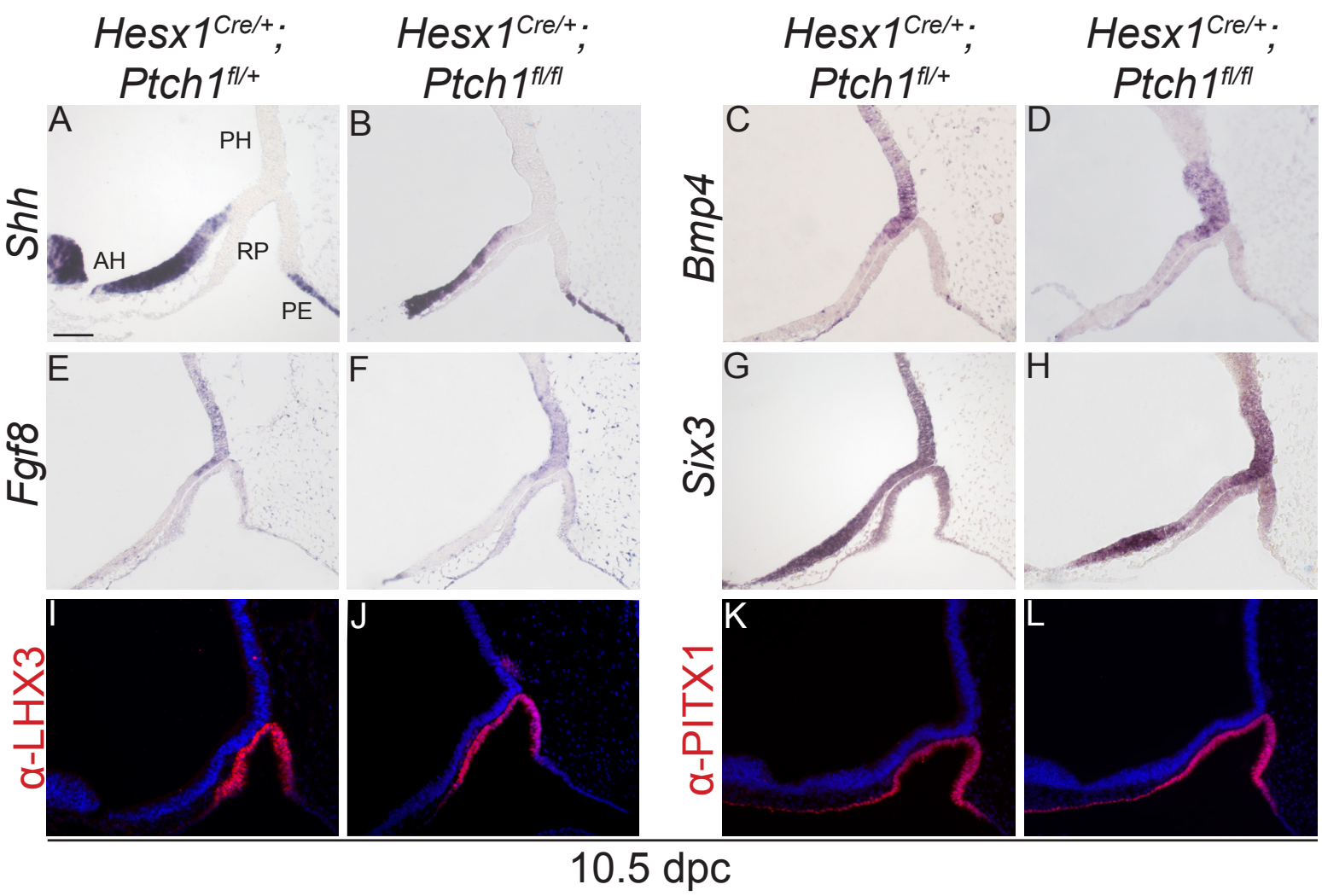

Figure S12. Patterning of the developing hypothalamus and Rathke's pouch is not affected in *Hesx1*$^{Cre/+}$;*Ptch1*$^{fl/fl}$ mutants. (A-L) *In situ* hybridisation (A-H) and immunofluorescence (I-L) on mid-sagittal sections of control and *Hesx1*$^{Cre/+}$;*Ptch1*$^{fl/fl}$ mutant embryos at 10.5 dpc. Markers are indicated. Note the comparable expression patterns of all markers analysed between genotypes. Abbreviations as in SFig. 2. Scale bar: 100μm

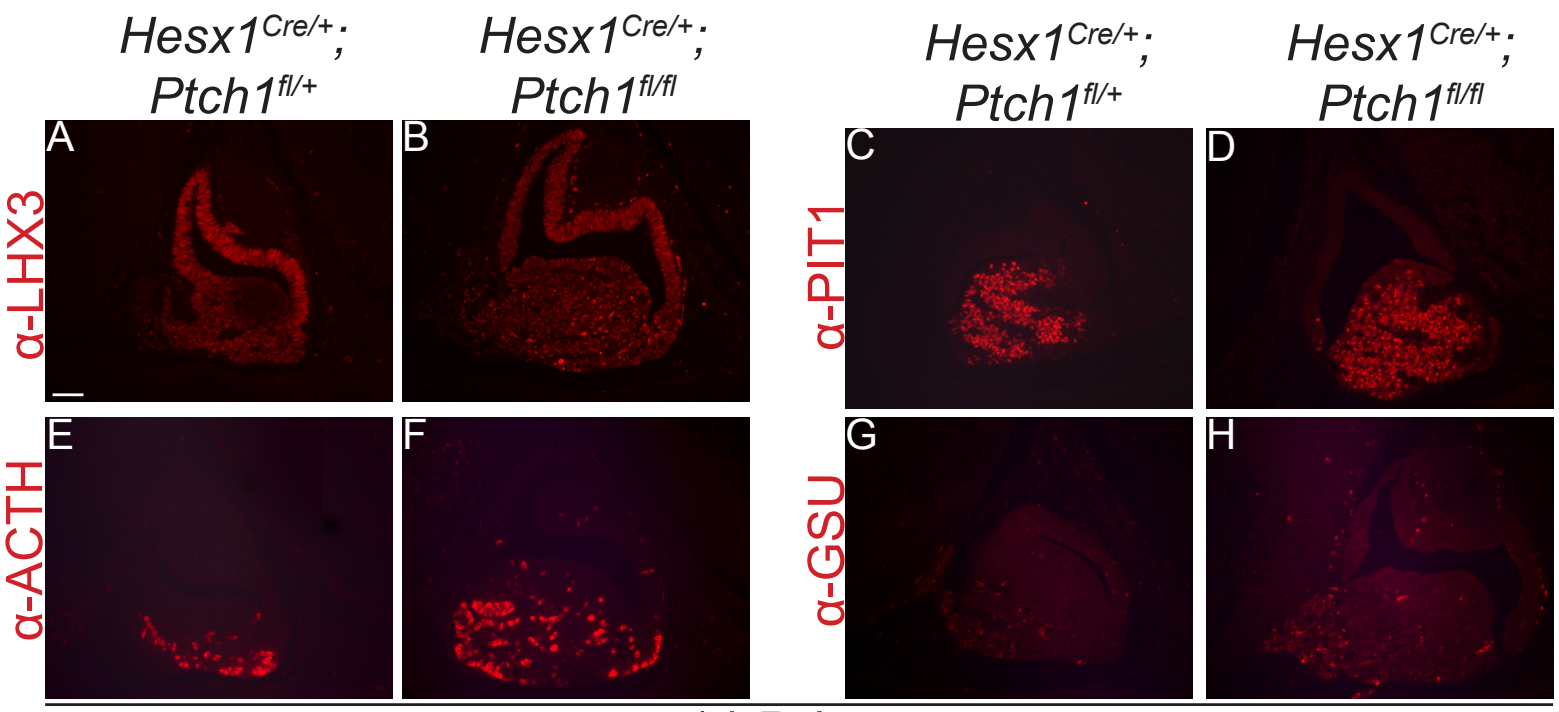

Figure S13. LHX3, ACTH, PIT1 and α-GSU are expressed in the developing pituitary of *Hesx1*$^{Cre/+}$;*Ptch1*$^{fl/fl}$ mutants. (A-H) Immunofluorescence on mid-sagittal histological sections of control and *Hesx1*$^{Cre/+}$;*Ptch1*$^{fl/fl}$ mutant embryos at 14.5 dpc. Note the enlargement of the expression domains of the markers analysed in the mutants relative to the control embryos. Scale bar: 100μm

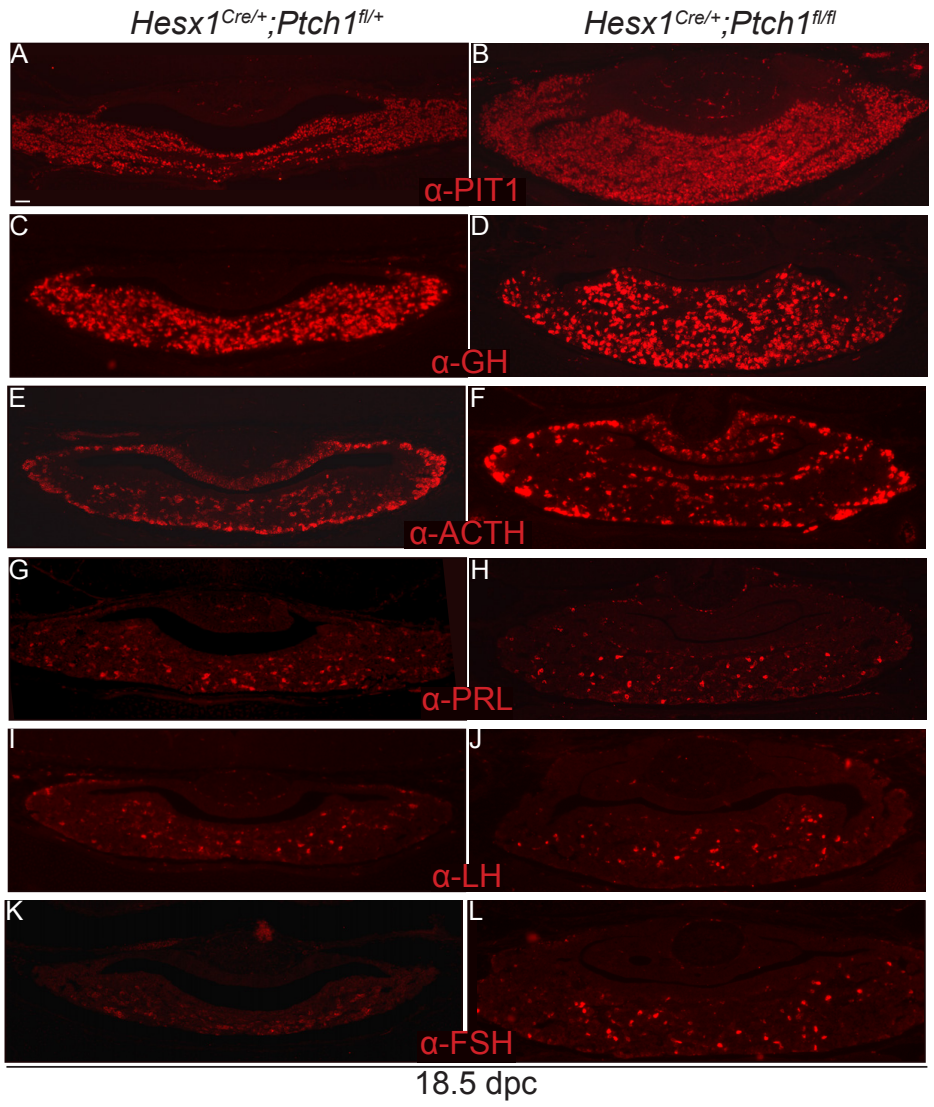

Figure S14. Hormone-producing cells are generated in the *Hesx1*$^{Cre/+}$;*Ptch1*$^{fl/fl}$ mutants at 18.5dpc. Immunofluorescence on frontal histological sections, at the level of the pituitary gland, in 18.5 dpc mutants and control embryos. Note the presence of PIT1+ve (somato, lacto and thyro -troph), GH+ve (somatotroph), ACTH+ve (cortico and melano -troph), PRL+ve (lactotrophs), LH+ve and FSH+ve (gonadotroph) cells in the mutant pituitary. Scale bars: 100μm.

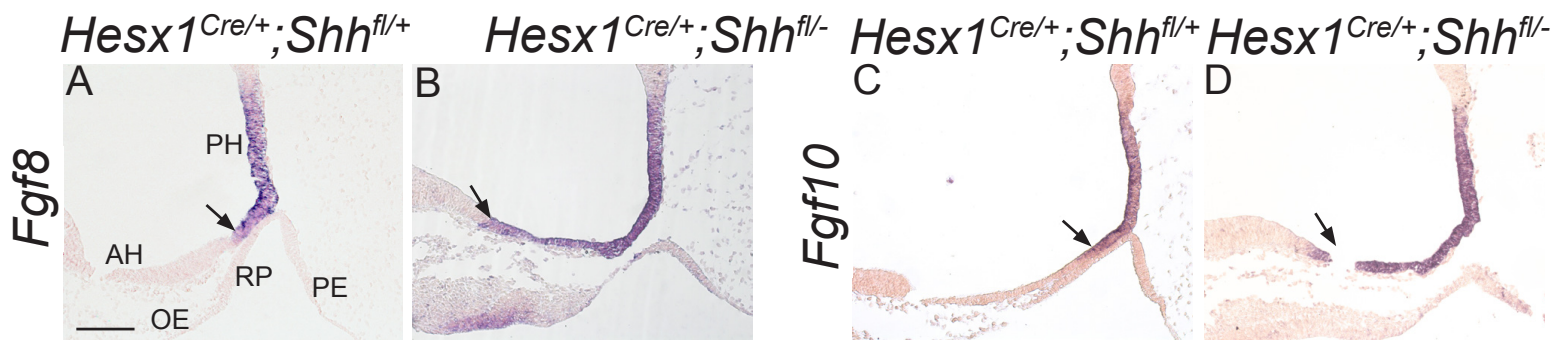

Figure S15. *Fgf8* and *Fgf10* are co-expressed in the developing hypothalamus. *In situ* hybridisation on mid-sagittal sections of *Hesx1*$^{Cre/+}$;*Shh*$^{fl/-}$ mutants and control embryos at 10.5 dpc. Note the co-expression of these two markers in the control and mutant embryos and the expansion of the *Fgf8/Fgf10* expression domains (arrows). Abbreviations as in SFig. 2.